AD-A035 510 PACIFIC-SIERRA RESEARCH CORP SANTA MONICA CALIF F/G 17/2.1
EFFECTS OF ANTENNA ELEVATION AND INCLINATION ON VLF/LF SIGNAL S--ETC(U)
DEC 76 E C FIELD, M LEWINSTEIN, M A DORE F19628-76-C-0157
UNCLASSIFIED PSR-612 RADC-TR-76-375 NL

1 OF 1
AD-A
035 510

END
DATE
FILMED
3-26-77
NTIS

EFFECTS OF ANTENNA EVALUATION AND INCLINATION ON VLF/LF SIGNAL STRUCTURE

PACIFIC-SIERRA RESEARCH CORPORATION
SANTA MONICA, CALIFORNIA

DECEMBER 1976

RADC-TR-76-375
Final Technical Report
December 1976

EFFECTS OF ANTENNA ELEVATION AND INCLINATION ON VLF/LF SIGNAL STRUCTURE

Pacific-Sierra Research Corporation

Approved for public release;
distribution unlimited.

ROME AIR DEVELOPMENT CENTER
AIR FORCE SYSTEMS COMMAND
GRIFFISS AIR FORCE BASE, NEW YORK 13441

SECURITY CLASSIFICATION OF THIS PAGE *(When Data Entered)*

REPORT DOCUMENTATION PAGE		READ INSTRUCTIONS BEFORE COMPLETING FORM
1. REPORT NUMBER RADC-TR-76-375	2. GOVT ACCESSION NO.	3. RECIPIENT'S CATALOG NUMBER
4. TITLE *(and Subtitle)* EFFECTS OF ANTENNA ELEVATION AND INCLINATION ON VLF/LF SIGNAL STRUCTURE		5. TYPE OF REPORT & PERIOD COVERED FINAL REPORT 1 Feb 1976 - 30 June 1976 6. PERFORMING ORG. REPORT NUMBER PSR-612
7. AUTHOR(s) E. C. Field, M. Lewinstein, and M.A. Dore		8. CONTRACT OR GRANT NUMBER(s) F19628-76-C-0157
9. PERFORMING ORGANIZATION NAME AND ADDRESS Pacific-Sierra Research Corporation 1456 Cloverfield Boulevard Santa Monica, California 90404		10. PROGRAM ELEMENT, PROJECT, TASK AREA & WORK UNIT NUMBERS Prog. Element 62101F Project Task, Work Unit Nos. 46031401
11. CONTROLLING OFFICE NAME AND ADDRESS Deputy for Electronic Technology (RADC) Hanscom AFB, Massachusetts 01731 Monitor/Paul Kossey/ETEE		12. REPORT DATE December, 1976 13. NUMBER OF PAGES 53
14. MONITORING AGENCY NAME & ADDRESS*(if different from Controlling Office)*		15. SECURITY CLASS. *(of this report)* Unclassified 15a. DECLASSIFICATION/DOWNGRADING SCHEDULE --

16. DISTRIBUTION STATEMENT *(of this Report)*

Approved for public release, distribution unlimited

17. DISTRIBUTION STATEMENT *(of the abstract entered in Block 20, if different from Report)*

18. SUPPLEMENTARY NOTES

19. KEY WORDS *(Continue on reverse side if necessary and identify by block number)*

VLF
Communications
Elevated antennas
Earth-ionosphere waveguide
Waveguide modes

20. ABSTRACT *(Continue on reverse side if necessary and identify by block number)*

This report analyzes the effects of antenna elevation and inclination on the structure of air-to-air VLF/LF communication signals for frequencies between 15 and 40 kHz. COnsidered are 1) propagation broadside to the horizontal component of trailing-wire transmitting antennas, and 2) ambient and moderately disturbed daytime ionospheric conditions and ground conductivities of 10^{-3} and 10^{-5} mhos/m. The calculations use full-wave methods, and fully account for the vertical inhomogeneity of the ionosphere

DD FORM 1 JAN 73 1473 EDITION OF 1 NOV 65 IS OBSOLETE

SECURITY CLASSIFICATION OF THIS PAGE *(When Data Entered)*

and the curvature of the earth. Numerical results are given for the excitation factors, height-gain factors, and attenuation rates of the first few TM and TE modes. Mode summations are carried out, and detailed plots are given for each field component versus distance for antenna altitudes between 0 and 40 kft.

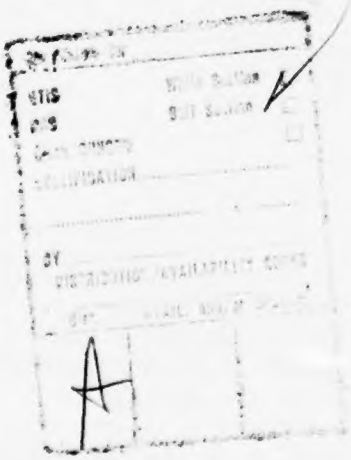

This report has been reviewed by the RADC Information Office (OI) and is releasable to the National Technical Information Service (NTIS). At NTIS it will be releasable to the general public, including foreign nations.

This technical report has been reviewed and approved for publication.

Approved: E. A. Lewis, Chief
VLF/ULF Techniques Branch

Approved: Allan C. Schell, Acting Chief
Electromagnetic Sciences Division

FOR THE COMMANDER

John P. Huss
Plans Office

SUMMARY AND CONCLUSIONS

This report analyzes the effects of antenna elevation and inclination on the structure of air-to-air VLF/LF communication signals for frequencies between 15 and 40 kHz. Considered are 1) propagation broadside to the horizontal component of trailing-wire transmitting antennas, and 2) ambient and moderately disturbed daytime ionospheric conditions and ground conductivities of 10^{-3} and 10^{-5} mhos/m. The calculations use full-wave methods, and fully account for the vertical inhomogeneity of the ionosphere and the curvature of the earth. Numerical results are given for the excitation factors, height-gain factors, and attenuation rates of the first few TM and TE modes. Mode summations are carried out, and detailed plots are given for each field component versus distance for antenna altitudes between 0 and 40 kft.

For ground-based antennas, the analysis shows that the vertical electric-field component associated with TM modes is dominant, even for electric-dipole antennas inclined as little as 10° with respect to the horizontal. For a moderate spread-debris nuclear environment, the vertically polarized component dominates the horizontally polarized component for all reasonable antenna inclinations, antenna elevations, and ranges beyond about 1500 km. This dominance occurs because of the high attenuation suffered by TE modes when ionospheric reflection-heights are severely depressed.

For ambient conditions--and presumably for weakly disturbed conditions--the horizontally polarized components associated with TE-mode propagation are dominant for antenna elevations of 25 kft or more, and antenna inclinations smaller than about 20°, measured from the horizontal.

PREFACE

This report analyzes the effects of antenna elevation and inclination on the structure of air-to-air VLF/LF communication signals for frequencies between 15 and 40 kHz. Ambient daytime and moderately disturbed ionospheric conditions are considered, as are ground conductivities of 10^{-3} and 10^{-5} mhos/m. The results are of interest to persons concerned with airborne antennas having significant horizontal components.

CONTENTS

		Page
SUMMARY AND CONCLUSIONS		1
PREFACE		2
SECTION I.	INTRODUCTION	6
II.	ELECTRIC DIPOLE FIELDS	7
	Excitation Factors	8
	Height-Gain Factors	12
	Attenuation Rates	18
	Field Strength versus Distance	21
III.	DISCUSSION	35
APPENDIX:	MATHEMATICAL SUMMARY	36
REFERENCES		48

FIGURES

Page

FIGURE 1. Excitation factor vs. frequency for lowest three TM modes (α=1,2,3) and lowest two TE modes (β=1,2): ambient day, $\sigma_g = 10^{-3}$ mhos/m 10

2. Height-gain factor for lowest three TM modes (α=1,2,3) and lowest two TE modes (β=1,2): 20 kHz, ambient day, $\sigma_g = 10^{-3}$ mhos/m 14

3. Height-gain factor for lowest three TM modes (α=1,2,3) and lowest two TE modes (β=1,2): 40 kHz, ambient day, $\sigma_g = 10^{-3}$ mhos/m 15

4. Height-gain factor for lowest two TM modes (α=1,2) and lowest two TE modes (β=1,2): 20 kHz, ambient day, $\sigma_g = 10^{-5}$ mhos/m 17

5. Attenuation rate vs. frequency for lowest three TM modes (α=1,2,3) and lowest two TE modes (β=1,2): ambient day, $\sigma_g = 10^{-3}$ mhos/m 19

6. Electric field strength vs. distance for ground-based and elevated VED and HED transmitters: 20 kHz, ambient day, $\sigma_g = 10^{-3}$ mhos/m 22

7. Magnetic field strength vs. distance for elevated VED and HED transmitters: 20 kHz, ambient day, $\sigma_g = 10^{-3}$ mhos/m 25

8. Electric field strength vs. distance for ground-based and elevated VED and HED transmitters: 40 kHz, ambient day, $\sigma_g = 10^{-3}$ mhos/m 27

9. Profiles of electric field strength at several distances from an HED transmitter 15 kft above the ground: 20 kHz, ambient day, $\sigma_g = 10^{-3}$ mhos/m 29

10. Electric field strength vs. distance for ground-based and elevated VED and HED transmitters: 20 kHz, ambient day, $\sigma_g = 10^{-5}$ mhos/m 30

11. Electric field strength vs. distance for ground-based and elevated VED and HED transmitters: 20 kHz, moderate spread-debris environment, $\sigma_g = 10^{-3}$ mhos/m 32

12. Electric field strength vs. distance for ground-based and elevated VED and HED transmitters: 40 kHz, moderate spread-debris environment, $\sigma_g = 10^{-3}$ mhos/m 33

13. Electric field strength vs. distance for elevated VED and HED transmitters: 20 kHz, ambient and disturbed ionospheres, $\sigma_g = 10^{-3}$ mhos/m 34

TABLES

		Page
TABLE 1.	Magnitudes of TM- and TE-Mode Excitation Factors at 20 kHz for Ambient Day and $\sigma_g = 10^{-5}$ mhos/m	11
2.	Magnitudes of Lowest TM- and TE-Mode Excitation Factors for a Moderate Spread-Debris Nuclear Environment, and $\sigma_g = 10^{-3}$ mhos/m	12
3.	TM- and TE-Mode Attenuation Rates at 20 kHz for Ambient Day and $\sigma_g = 10^{-5}$ mhos/m	21
4.	Lowest TM- and TE-Mode Attenuation Rates for a Moderate Spread-Debris Nuclear Environment and $\sigma_g = 10^{-3}$ mhos/m	21

I. INTRODUCTION

Propagation of very-low-frequency (VLF) and low-frequency (LF) signals between airborne terminals is much more complicated than for ground-based links, where only transverse-magnetic (TM) waveguide modes need be considered for long-range communications. An antenna at an altitude of several kilometers can radiate, or receive, horizontally polarized transverse-electric (TE) modes with reasonable efficiency. Moreover, for high-speed aircraft, trailing-wire antennas have a nearly horizontal orientation, and are therefore inherently better coupled to horizontally polarized signals than to vertically polarized ones. Thus, TE modes in the earth-ionosphere waveguide cannot be neglected for elevated antennas, and the received signal will be a complicated combination of TM and TE modes.

This report analyzes the effects of antenna elevation and inclination on the structure of air-to-air VLF/LF communication signals. Propagation broadside to the horizontal component of trailing-wire transmitting antennas is considered, and results are presented for ambient daytime and moderately disturbed ionospheric conditions, and ground conductivities of 10^{-3} and 10^{-5} mhos/m. For these ionospheric environments, the effects of the geomagnetic field can be (and are) neglected. Numerical calculations are made of excitation factors, height-gain factors and attenuation rates of the first few TM and TE modes, and detailed plots are given for each field component versus distance for antenna altitudes between 0 and 40 kft. The numerical results are given in Sec. II, and the equations used are given in the appendix.

II. ELECTRIC DIPOLE FIELDS

The fields of an electric dipole in the earth-ionosphere waveguide can be expressed as summations of elementary waveguide modes--so-called TM and TE modes. For daytime or disturbed conditions, when geomagnetic mode-coupling can be neglected, the vertical electric dipole (VED) excites only TM modes. Each TM mode, and hence the total VED field, contains only three components;* *viz*, the radial (or vertical) electric field, E_r^V, the transverse magnetic field, H_ϕ^V, and the longitudinal electric field, E_θ^V. The horizontal electric dipole (HED) excites both TM and TE modes and, for arbitrary orientations, excites all six field components. However, for propagation perpendicular to the dipole axis--the situation analyzed in this report--only the radial (vertical) magnetic field H_r^H, the transverse electric field, E_ϕ^H, and the longitudinal magnetic field, H_θ^H, are excited. Although these are the same three field components that are present in a pure TE mode, the HED broadside fields are, in fact, composed of complicated combinations of both TE and TM modes. This absence of pure modal excitation has led to the nomenclature "quasi-modes" for the HED fields.

The rather complex expressions for the fields are given in the appendix, as are the equations and numerical procedures used to obtain the parameters characterizing the various modes. The contribution of each mode to the total field is proportional to the product of four factors; *viz*, the excitation factor, the transmitter height-gain

---

*Conventional spherical coordinates are used, as are MKS units. The transmitter is at $\theta = 0$, the waves propagate in the θ direction, the path is at an azimuthal angle, ϕ, and the HED axis is in the $\phi = 0$ direction.

factor, the receiver height-gain factor, and the propagation factor. Numerical results for each of these factors for several modes, as well as for the total VED and HED fields, are given below. Earth conductivities, σ_g, of 10^{-3} and 10^{-5} mhos/m are considered. Most of the results are for a nominal daytime ionosphere, approximated by an exponential conductivity height-gradient ($\beta = 0.5$, $H = 70$ km, in *Wait's 1970* nomenclature;* see appendix). For comparison, some results are given for a "moderate" spread-debris nuclear environment ($W = 2\text{x}10^{-10}$ in the nomenclature of *Field and Dore, 1975*,** who give ionization and collision-frequency height-profiles).

EXCITATION FACTORS

The strength with which a given mode is excited by a *ground-based* transmitter is accounted for by the excitation factor, A. Usually, the VLF excitation factor is normalized to unity for TM-mode excitation by a VED in an idealized, sharply bounded earth-ionosphere waveguide. This normalization is accomplished by factoring out the "height of the ionosphere," which is well defined under the assumption of a sharply bounded ionosphere (*Galejs, 1972*).*** This factorization cannot be made in our treatment, since, in our use of arbitrarily continuous ionospheric height-profiles, the artifact of an "ionospheric height" never appears in the equations. Consequently, the excitation factors

---

*J. R. Wait, *Electromagnetic Waves in Stratified Media*, Pergamon Press, New York, 1970.

**E. C. Field, and M. Dore, *VLF/LF TE-Mode Propagation Under Disturbed Ionospheric Conditions*, Air Force Cambridge Research Laboratories, AFCRL-TR-75-0382, July 1975.

***J. Galejs, *Terrestial Propagation of Long Electromagnetic Waves*, Pergamon Press, New York, 1972.

computed here have units of inverse distance, and differ in magnitude from those of other authors (*Wait and Spies, 1964;*[*] *Galejs, 1972*) by a factor corresponding roughly to the "ionospheric heights" at which important reflections occur. (See appendix.) These heights are, of course, ill-defined for a realistic diffuse ionosphere, and depend on frequency, mode number, and ionospheric model. However, our excitation factors, for example, are smaller than those of Wait and Galejs by a factor of $(6\text{x}10^4 - 7\text{x}10^4\ \text{m})^{-1}$ for VLF and nominal daytime conditions.

Figure 1 shows the frequency dependence of the excitation-factor magnitudes of the first three TM modes ($\alpha = 1,2,3$) and first two TE modes ($\beta = 1,2$) for ambient daytime conditions and $\sigma_g = 10^{-3}$ mhos/m. (A ground dielectric constant of 10 is assumed in all calculations in this report.) The important thing to note from Fig. 1 is the *relative* magnitudes of the various modes, since these magnitudes give the relative contribution of each mode to the total fields at short distances from ground-based electric dipoles. Effects of elevation and long-path propagation are accounted for in the height-gain and propagation factors, to be given later. At the lower frequencies, multiplying A_α by nominal reflection heights of 6×10^4 to 7×10^4 m gives a result near unity, as discussed earlier.

The first three TM modes (denoted by "α") are excited about equally at the lower VLF frequencies, but, above about 30 kHz, the higher-order TM modes are much more effectively excited than the first one. The TE modes (denoted by "β") are excited much more poorly than

---

[*] J. R. Wait, and K. P. Spies, *Characteristics of the Earth-Ionosphere Waveguide for VLF Radio Waves*, U.S. Department of Commerce, National Bureau of Standards, Tech. Note 300, 1964.

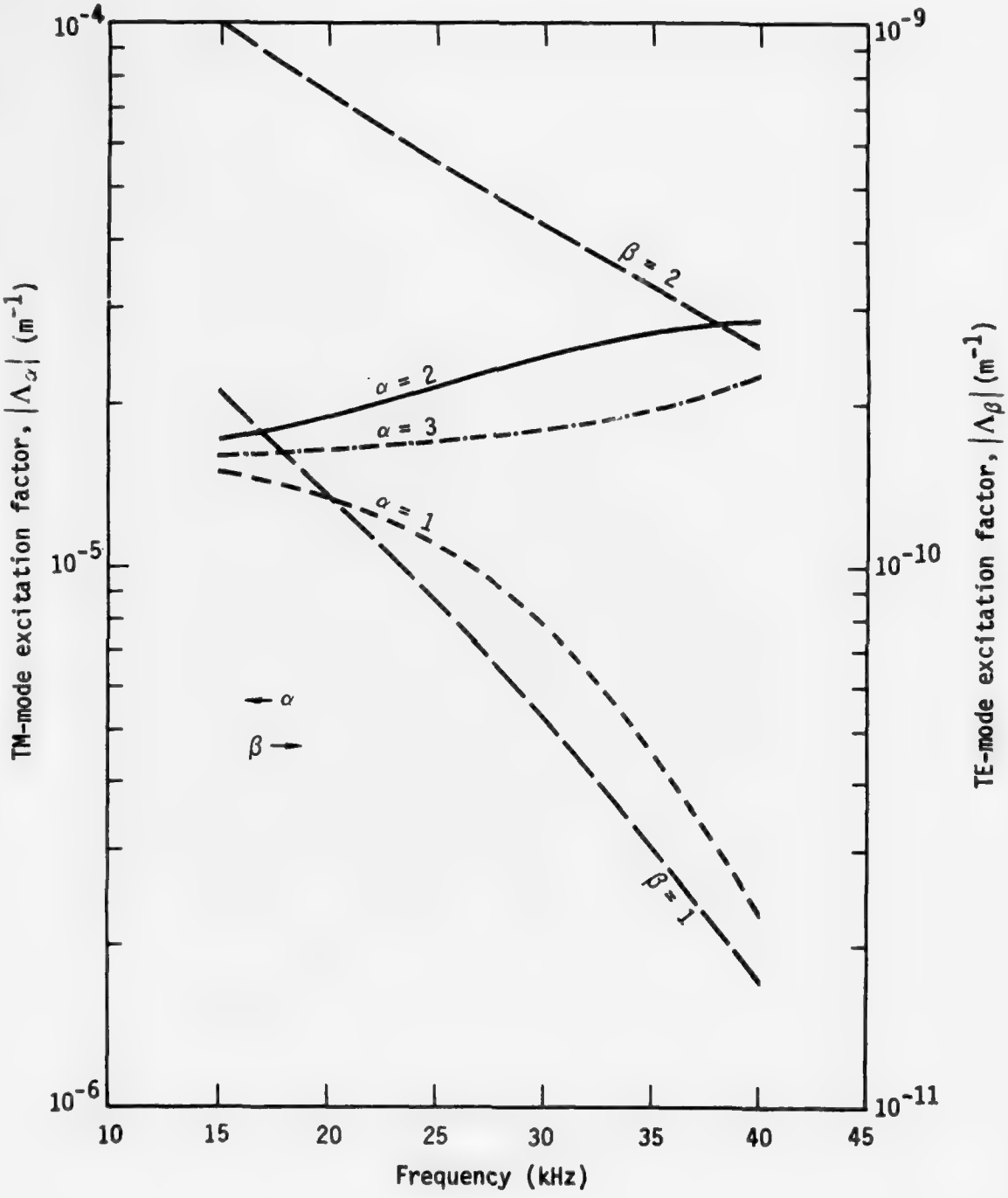

Figure 1. Excitation factor vs. frequency for lowest three TM modes (α=1,2,3) and lowest two TE modes (β=1,2): ambient day, $\sigma_g = 10^{-3}$ mhos/m.

the TM modes, as shown by the fact that A_α exceeds A_β by four or five orders of magnitude. This behavior corresponds to the well-known inability of transmitters on highly conducting grounds to effectively radiate TE waves at low frequencies. As was the case for TM modes, the second TE mode is more effectively excited than the first.

The efficiency of TE-mode excitation relative to TM-mode excitation improves as the ground conductivity is reduced. Table 1 shows the magnitude of the excitation factors for the first two TM and TE modes at 20 kHz for ambient daytime conditions and $\sigma_g = 10^{-5}$ mhos/m. The TE-mode excitation factors are nearly two orders of magnitude greater for $\sigma_g = 10^{-5}$ mhos/m than for $\sigma_g = 10^{-3}$ mhos/m. On the other hand, comparison of Table 1 with Fig. 1 shows that the lowest TM mode is much more poorly excited for $\sigma_g = 10^{-5}$ mhos/m than for 10^{-3} mhos/m.

TABLE 1. MAGNITUDES OF TM- AND TE-MODE EXCITATION FACTORS AT 20 kHz FOR AMBIENT DAY AND $\sigma_g = 10^{-5}$ mhos/m

1st TM ($\alpha = 1$)	2nd TM ($\alpha = 2$)	1st TE ($\beta = 1$)	2nd TE ($\beta = 2$)
2.4×10^{-6}	9.6×10^{-5}	9.4×10^{-9}	5.2×10^{-8}

The excitation factor also depends on the state of the ionosphere. As indicated above and in the appendix, the excitation factors as defined here are inversely proportional to a quantity that becomes the "height of the ionosphere" in the limit of a sharply bounded ionosphere. For the diffuse ionospheres used here, the excitation factors at the lower VLF frequencies are roughly proportional to the inverse of the average height at which important reflections occur. Thus, one

would expect these factors to become somewhat larger under disturbed conditions, where the ionosphere is significantly depressed. Table 2 gives calculated excitation factors for a moderate spread-debris nuclear environment (i.e., $W = 2 \times 10^{-9}$; see *Field and Dore, 1975*) and $\sigma_g = 10^{-3}$ mhos/m. Comparison of Table 2 with Fig. 1 shows that the excitation of the lower TE and TM modes at 20 and 40 kHz is increased by the disturbance. Results are shown only for the first modes because the higher modes are so heavily attenuated as to be unimportant at useful communication distances.

TABLE 2. MAGNITUDES OF LOWEST TM- AND TE-MODE EXCITATION FACTORS FOR A MODERATE SPREAD-DEBRIS NUCLEAR ENVIRONMENT, AND $\sigma_g = 10^{-3}$ mhos/m

Frequency	1st TM ($\alpha = 1$)	1st TE ($\alpha = 1$)
20 kHz	2.4×10^{-5}	6.0×10^{-10}
40 kHz	2.6×10^{-5}	3.5×10^{-10}

HEIGHT-GAIN FACTORS

The height-gain factor of a waveguide mode accounts for the effects of nonzero transmitter and receiver heights. More precisely, the transmitter height-gain factor is the ratio of the mode excitation for the actual transmitter height, h, to the mode excitation for a ground-based transmitter. Similarly, the receiver height-gain factor is the ratio of the mode strength at the receiver height, z, to the mode strength at the ground. Physically, the TM-mode height-gain factors are equal to the height-profiles of the transverse magnetic fields, $H_{\phi\alpha}$, normalized to unity at the ground, whereas the TE-mode

height-gain factors are the height-profiles of the transverse electric fields, $E_{\phi\beta}$, normalized to unity at the ground.

The manner in which the height-gain factors enter the field equations is shown in detail in the appendix. But, the salient point is as follows: For elevated terminals, the contribution of a mode to the total field is proportional to the product of the excitation factor, the transmitter height-gain factor, and the receiver height-gain factor. The transmitter and receiver height-gain factors of a given mode are functionally identical and, therefore, are equal when transmitter and receiver are at the same altitude. In this case, the relative importance of a mode is proportional to the product of the excitation factor and the square of the height-gain factor computed for the appropriate altitude.

Figures 2 and 3 show height-gain factors G_α and G_β for the first three TM modes ($\alpha = 1,2,3$) and first two TE modes ($\beta = 1,2$) for ambient daytime conditions, $\sigma_g = 10^{-3}$ mhos/m, and frequencies of 20 and 40 kHz. These height-gain factors exhibit the classic height-dependences for antennas over a highly conductive ground; *viz*, the TM-mode height-gain factors are of order unity over most of the waveguide, except for some rather sharp nulls; above a few kilometers, the TE-mode height-gain factors increase sharply to values over 100.

For elevated antennas, the large TE-mode height-gain factor mitigates the effects of the small excitation factor, and these modes can be excited about as effectively as TM modes. Stated mathematically, for altitudes where the height-gain factors have achieved nearly their maximum value, the quantity $\Lambda_\beta G_\beta^2$ is of the same order of magnitude as

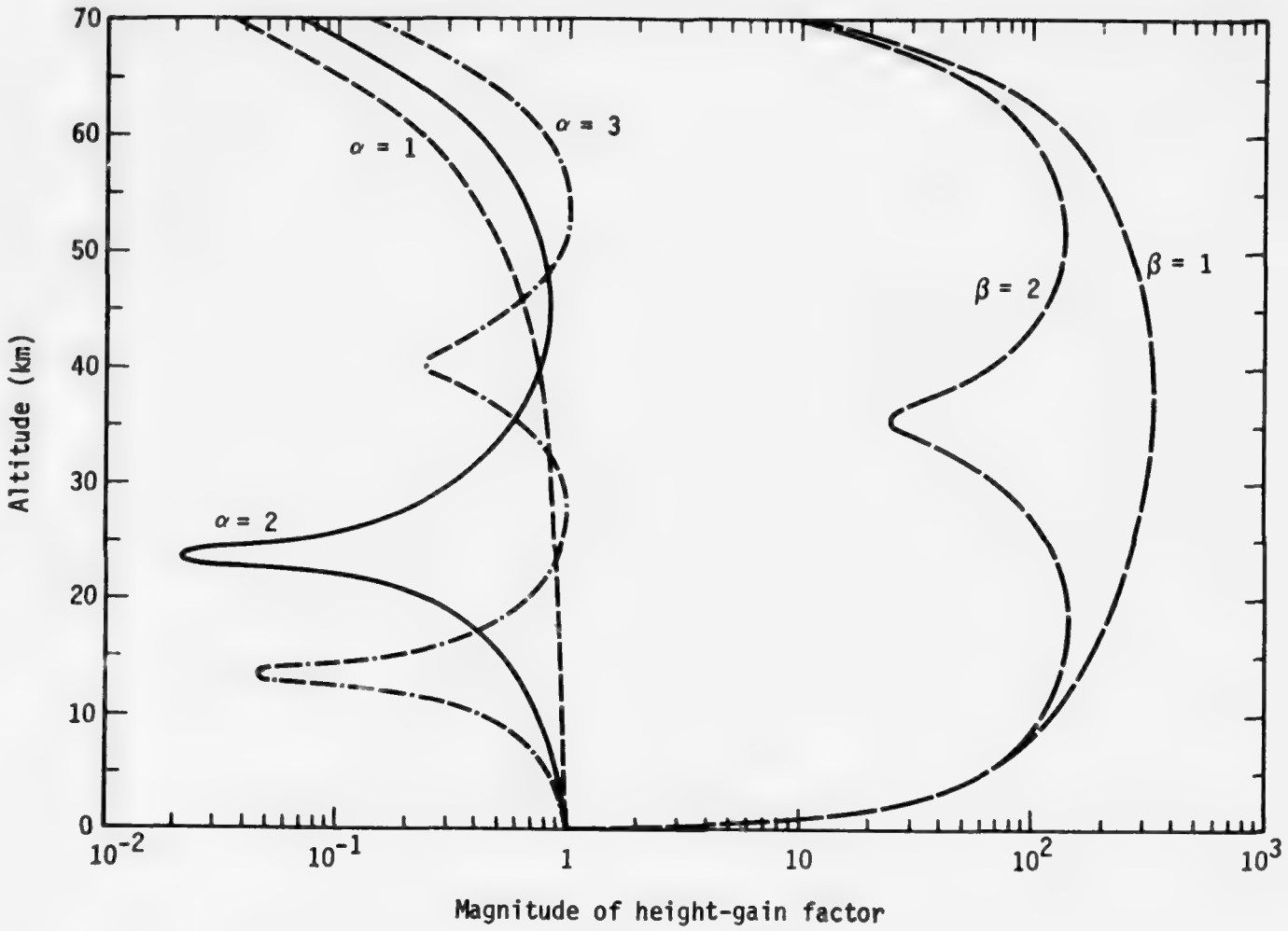

Figure 2. Height-gain factor for lowest three TM modes (α=1,2,3) and lowest two TE modes (β=1,2): 20 kHz, ambient day, σ_g = 10^{-3} mhos/m.

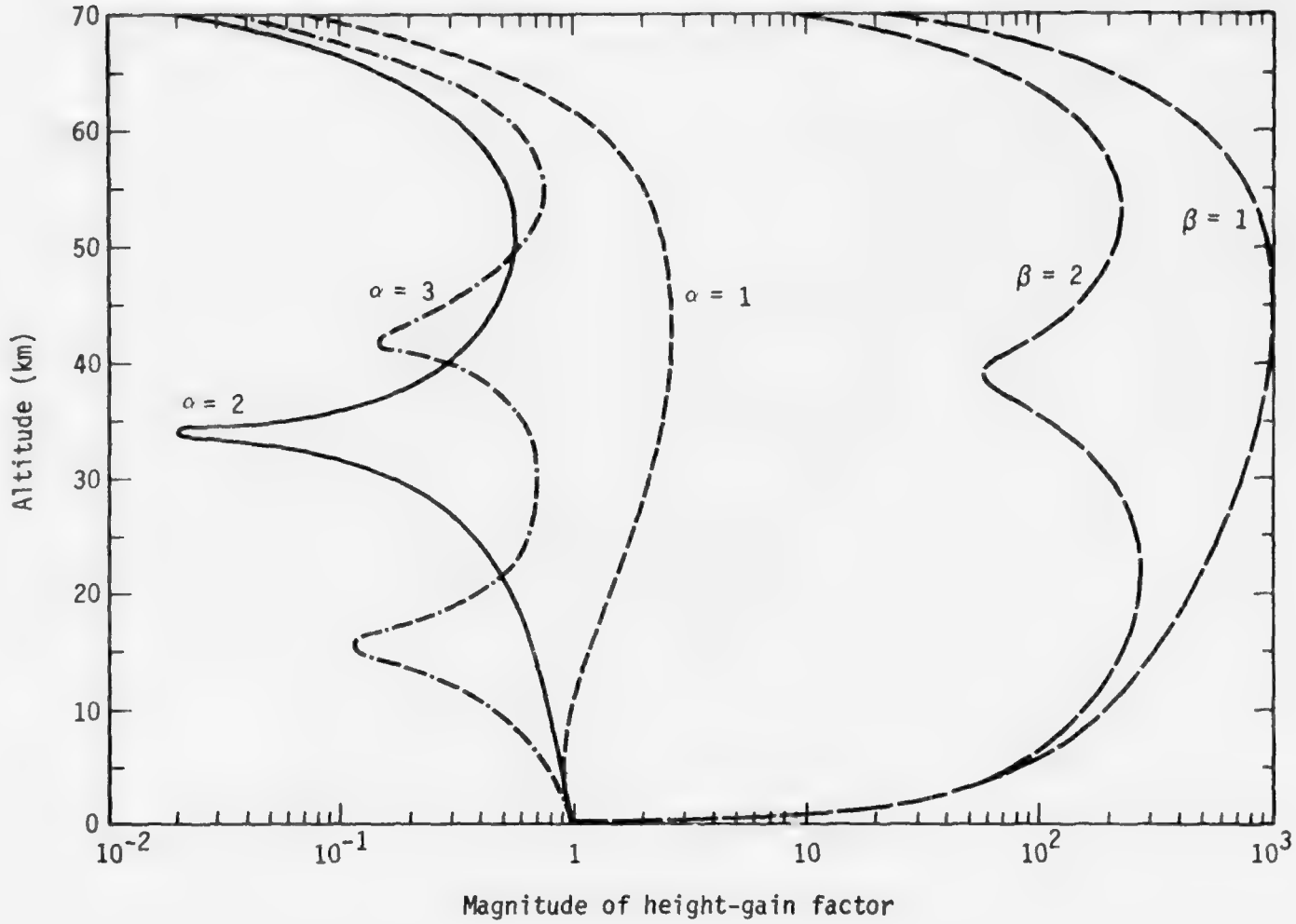

Figure 3. Height-gain factor for lowest three TM modes (α=1,2,3) and lowest two TE modes (β=1,2): 40 kHz, ambient day, $\sigma_g = 10^{-3}$ mhos/m.

the quantity $\Lambda_\alpha G_\alpha^2$. Numerical values from Figs. 1 through 3 can be used to confirm this fact, as can the relationships

$$\Lambda_\alpha = \left[2 \int_a^\infty \frac{G_\alpha^2(r)dr}{n^2(r)} \right]^{-1} \quad , \quad \Lambda_\beta = \left[2 \int_a^\infty G_\beta^2(r)dr \right]^{-1}$$

(appendix, Eqs. (A26) and (A37)), which guarantees that large height-gain factors are associated with small excitation factors, and vice versa. In the above equations, a is the earth's radius, and n^2 is the ionospheric refractive index. Figures 2 and 3 show that, even for aircraft altitudes of 5 to 10 km, the TE-mode height-gain factors become very large, albeit well below their peak values.

Note that, at 40 kHz, the first TM mode shows some tendency toward the characteristics of the so-called earth-detached or "whispering gallery" modes, which have most of their energy concentrated at the base of the ionosphere. The case shown is not particularly striking, since the peak of the $\alpha = 1$ height-gain factor at 45 to 50 km is only about three. However, at higher frequencies--say, 70 to 100 kHz--the first TM height-gain factor can become larger than 100 just below the ionosphere, thereby exhibiting true "whispering gallery" characteristics (*Galejs, 1972*). The use of only a few waveguide modes to characterize 70- to 100-kHz waves is invalid for most conditions.

Figure 4 shows the height-gain factors of the lowest two TM and TE modes for ambient day, $\sigma_g = 10^{-5}$ mhos/m, and a frequency of 20 kHz. Comparison with Fig. 2 (p. 14) shows that the shapes of the TE-mode height-gains are virtually unchanged by the two-orders-of-magnitude reduction in ground conductivity, but the peak values of the

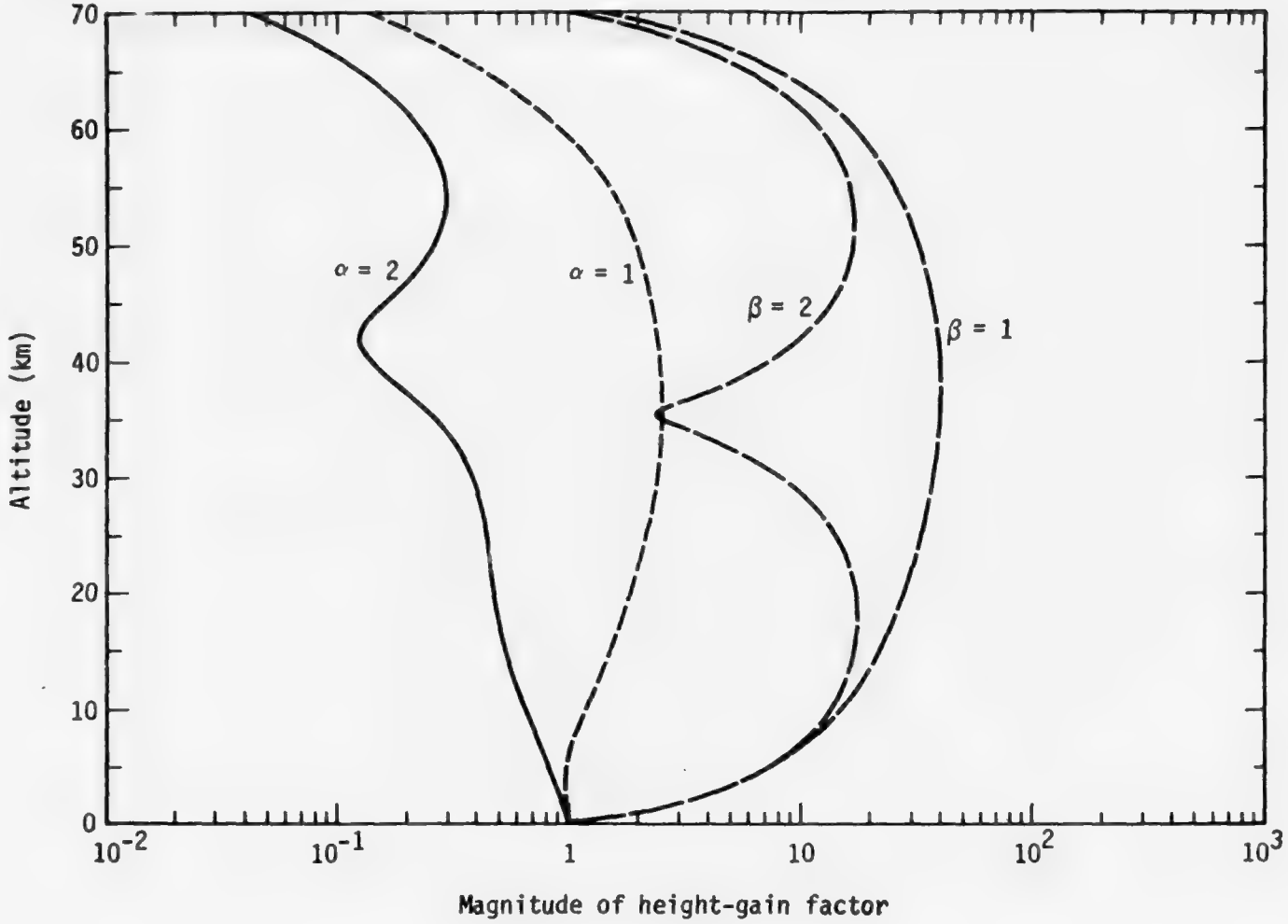

Figure 4. Height-gain factor for lowest two TM modes (α=1,2) and lowest two TE modes (β=1,2): 20 kHz, ambient day, σ_g = 10^{-5} mhos/m.

height-gains are reduced by an order of magnitude. This behavior is consistent with the two-orders-of-magnitude increase in excitation factor discussed above, since Λ_β tends to be proportional to $1/\sigma_g$, and G_β tends to be proportional to $\sigma_g^{1/2}$ (*Galejs, 1972*). The main effect of the change in ground conductivity on the TM-mode height-gain is a relatively minor change in shape, which causes the $\alpha = 1$ mode to have slight earth-detached properties.

ATTENUATION RATES

Modal attenuation rates account for the reduction--over and above cylindrical spreading--in strength suffered by a mode in propagating between transmitter and receiver. Figure 5 shows calculated attenuation rates versus frequency for the first three TM modes and the first two TE modes for ambient daytime conditions and $\sigma_g = 10^{-3}$ mhos/m. The higher-order modes are more heavily attenuated than the lower-order ones, which allows one to neglect the higher terms in the mode sums at large distances. At 40 kHz, however, the attenuation rates for the TE modes differ by only about 2 dB/Mm. Given that the higher modes are more effectively excited than are lower ones, it is doubtful that the mode sum can be truncated throughout the upper LF band under ambient conditions. In this case, ray tracing is a better approach to the propagation analysis. For moderately disturbed conditions, the higher modes are much more heavily attenuated than the first modes, and the mode sum can be used well into the LF regime.

Figure 5 shows that the lowest TE mode is slightly less attenuated than the lowest TM mode. This behavior is in contrast to results given by Field and Dore (*1975*) for a perfectly conducting ground, and an

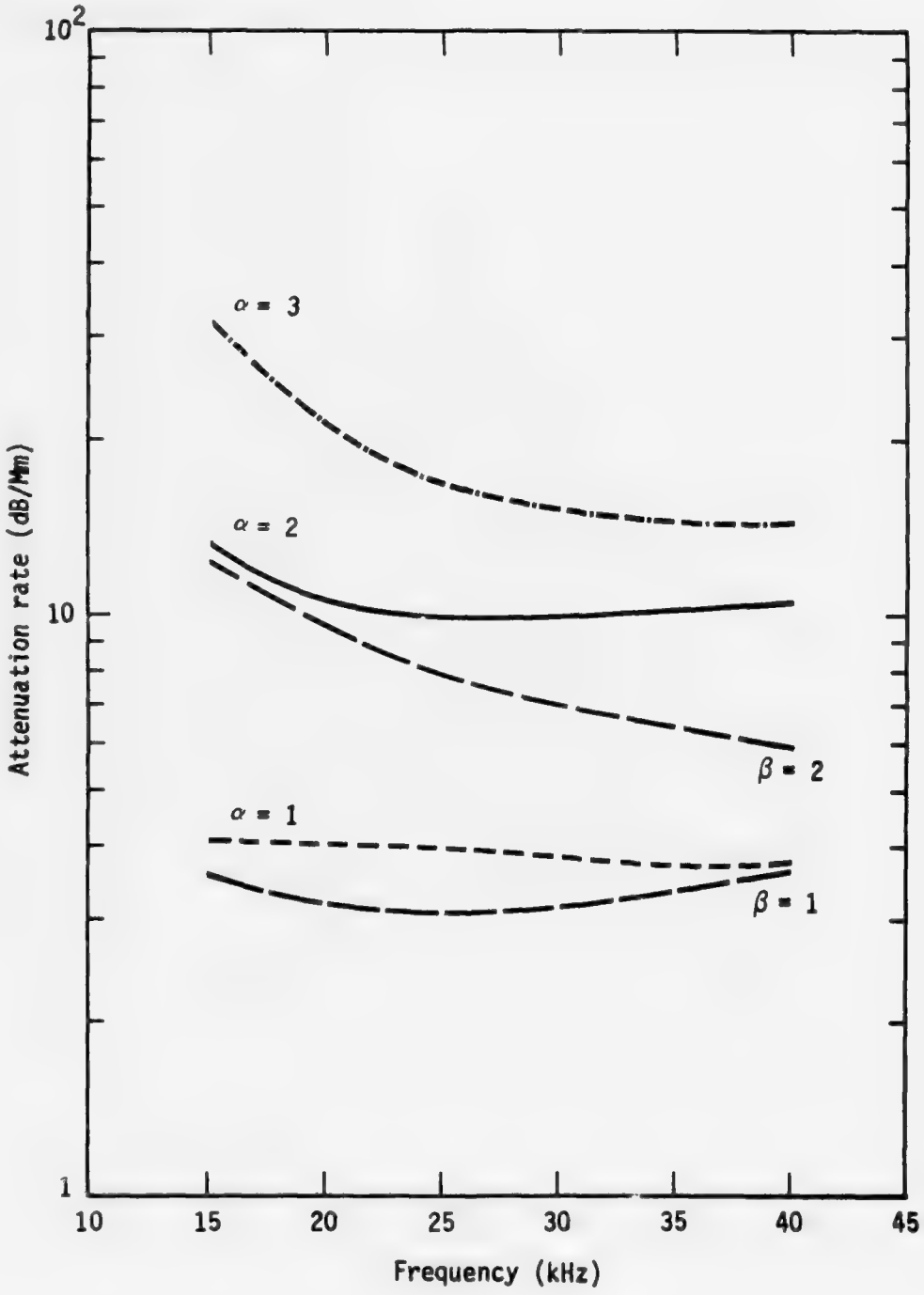

Figure 5. Attenuation rate vs. frequency for lowest three TM modes (α=1,2,3) and lowest two TE modes (β=1,2): ambient day, $\sigma_g = 10^{-3}$ mhos/m.

ambient daytime model ionosphere that differs slightly from the one used here. Those results indicated that the first TM-mode attenuation rate was between 2 and 3 dB/Mm, which was 1 or 2 dB/Mm less than the lowest TE-mode attenuation rate. The decrease in assumed ground conductivity from ∞ to 10^{-3} mhos/m causes the first TM-mode attenuation to essentially double, while the TE-mode attenuation is relatively unaltered.

In addition to the results given in Fig. 5, some attenuation rates have been calculated for ambient day with $\sigma_g = 10^{-5}$ mhos/m, and a moderate ($W = 2 \times 10^{-9}$) spread-debris nuclear environment with $\sigma_g = 10^{-3}$ mhos/m. The results are shown in Tables 3 and 4. Comparison of Table 3 with Fig. 5 shows that the TE-mode attenuation rate is relatively insensitive to ground conductivity, being only slightly larger for $\sigma_g = 10^{-5}$ mhos/m than for $\sigma_g = 10^{-3}$ mhos/m. On the other hand, the TM-mode attenuation rates become quite large for $\sigma_g = 10^{-5}$ mhos/m. This behavior agrees with the results of Pappert (*1970*),* and occurs because the TM reflection coefficient has a quasi-Brewster angle effect at the ground, whereas the TE coefficient does not. Comparison of Table 4 with Fig. 5 shows that both TM- and TE-mode attenuation rates are drastically increased by the disturbance, with the TE modes becoming much more highly attenuated than the TM modes. This behavior is consistent with that computed by Field and Dore (*1975*) for infinite ground conductivity.

In summary, TM-mode attenuation rates are more sensitive to changes in ground conductivity than are TE-mode attenuation rates, but TE modes are relatively more sensitive to ionospheric disturbances.

---

*R. A. Pappert, "Effects of Elevation and Ground Conductivity on Horizontal Dipole Excitation of the Earth-Ionosphere Waveguide," *RADIO Science*, Vol. 5, No. 3, March 1970, pp. 579-590.

TABLE 3. TM- AND TE-MODE ATTENUATION RATES AT 20 kHz FOR AMBIENT DAY AND $\sigma_g = 10^{-5}$ mhos/m

1st TM ($\alpha = 1$)	2nd TM ($\alpha = 2$)	1st TE ($\beta = 1$)	2nd TE ($\beta = 2$)
8.6 dB/Mm	87 dB/Mm	3.4 dB/Mm	10.9 dB/Mm

TABLE 4. LOWEST TM- AND TE-MODE ATTENUATION RATES FOR A MODERATE SPREAD-DEBRIS NUCLEAR ENVIRONMENT AND $\sigma_g = 10^{-3}$ mhos/m

Frequency	1st TM ($\alpha = 1$)	1st TE ($\alpha = 1$)
20 kHz	11.2 dB/Mm	24.9 dB/Mm
40 kHz	13.2 dB/Mm	19.0 dB/Mm

FIELD STRENGTH VERSUS DISTANCE

The main ingredients used in forming the mode sums--the excitation, height-gain, and attenuation factors--have been given above. Of course, the phase of these quantities, as well as the magnitudes, have been used in our calculations. The formulas used to calculate the VED and HED field components are given in the appendix.

Figure 6 gives the electric field components versus distance for ambient day, $\sigma_g = 10^{-3}$ mhos/m, and a frequency of 20 kHz. The superscripts V and H denote VED and HED, respectively. The VED fields are independent of azimuth, whereas the HED fields are calculated for broadside ($\phi = \pi/2$) propagation. The first three TM modes are included in the VED mode summation, whereas the first three TM modes *and* the

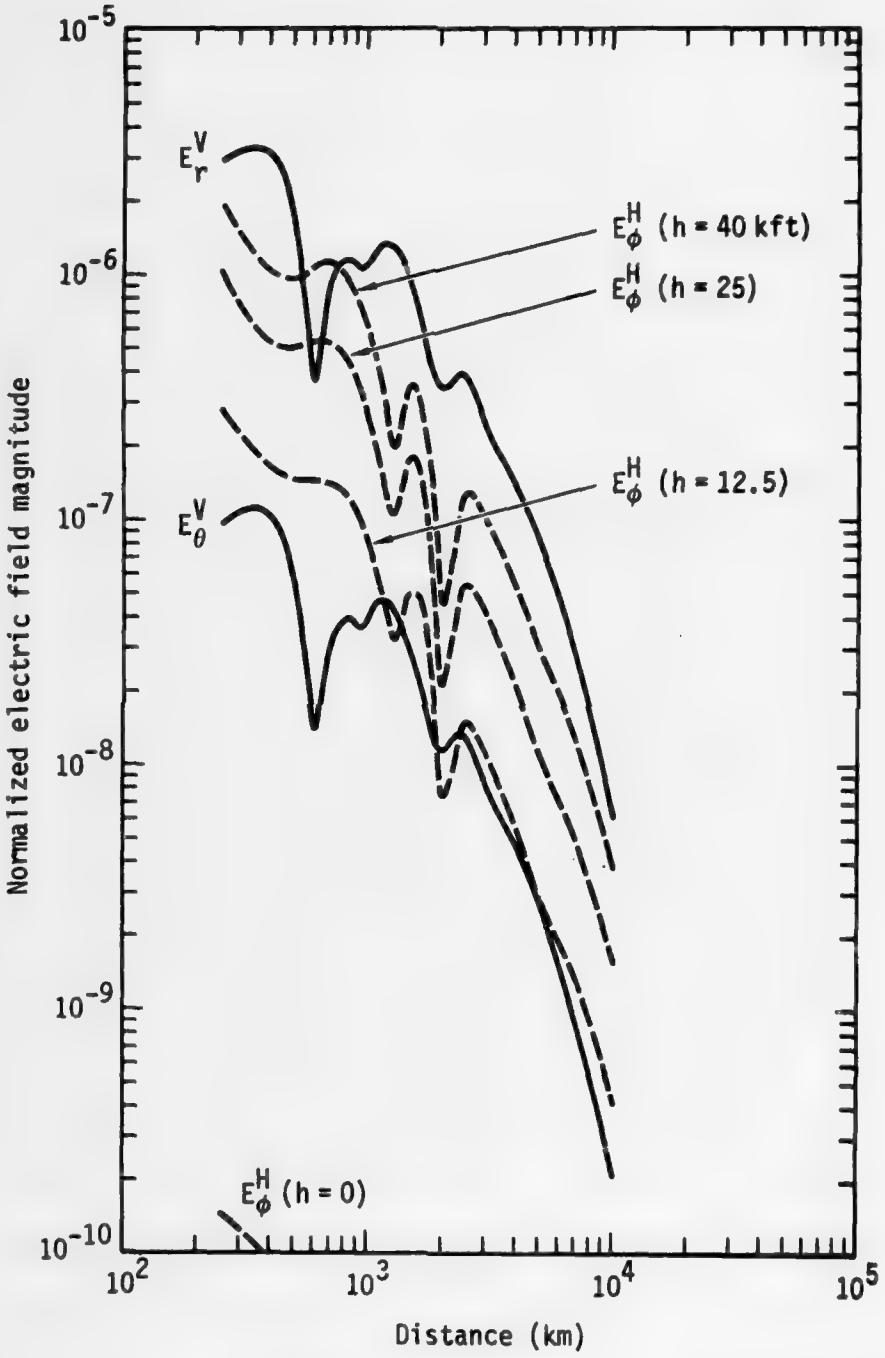

Figure 6. Electric field strength vs. distance for ground-based and elevated VED and HED transmitters: 20 kHz, ambient day, $\sigma_g = 10^{-3}$ mhos/m.

first two TE modes are included in the HED mode summation. Additional modes would have little effect on the results shown in Fig. 6.

All electric field strengths in this report have been normalized so that

$$I\ell Z_o/\lambda = 1 \text{ volt} \quad ,$$

where I is the transmitting antenna current, ℓ is the effective antenna length, λ is the free-space wavelength, and Z_o is the free-space impedance. To obtain actual field strengths in volts/meter, the curves given in this report should be multiplied by the actual value of $I\ell Z_o/\lambda$.

As can be inferred from Figs. 2 through 4 (pp. 14, 15, and 17), the lowest TM-mode fields and, hence, the VED fields, do not depend strongly on height for typical aircraft altitudes of, say, 15 km or less. Thus, E_r^V and E_θ^V are shown in Fig. 6 (and in subsequent figures) for the case where both transmitting and receiving antenna are on the ground. The fields for realistic airborne-antenna heights differ only slightly from those shown. The HED fields, on the other hand, contain TE modes, which depend very strongly on antenna altitude. HED field strengths are therefore shown for four cases; *viz*, when *both* transmitter and receiver are at altitudes of 0, 12.5, 25, and 40 kft.

The VED and HED fields shown in Fig. 6 (and in subsequent figures) are directly comparable only when both transmitting and receiving antennas have equal horizontal and vertical components; i.e., when trailing-wire antennas have inclination angles of 45°. If trailing-wire transmitting and receiving antennas inclined 10° to the horizontal are used, E_r^V must be reduced by $\sin^2 10°/\cos^2 10° \approx 3 \times 10^{-2}$ relative

to E_ϕ^H, and E_θ^V must be reduced by sin 10°/cos 10° ≈ 0.17 relative to E_ϕ^H, in order to compare received signal strengths.

As would be expected, the fields of the ground-based HED are orders of magnitude below those of the VED, and are therefore unusable. The comparison is much more favorable for elevated antennas, however, where E_r^V exceeds E_ϕ^H by a factor of 5 or 10 at h = 25 kft, and a factor of only 2 or 3 at h = 40 kft. After the factor of 3×10^{-2} adjustment is made for 10° inclinations of transmitting and receiving antennas, the HED signal is between 20 and 25 dB stronger than the VED signal for an antenna elevation of 40 kft.

Figure 7 is a companion to Fig. 6, and shows the VED and HED magnetic intensities for antenna altitudes of 40 kft. The normalized intensities $H = Z_o H$ are used so that the magnetic and electric fields are directly comparable. In fact, comparison of Figs. 6 and 7 shows that the results are essentially identical, provided the substitutions $E_r^V \to H_\phi^V$ and $E_\phi^H \to H_r^H$ are made. Thus, subsequent results need be shown only for the electric fields. The fact that $E_\phi^H \approx H_r^H$ shows that the HED broadside fields are dominated by the TE modes in the mode sum.

If loop receivers are used to sense the magnetic field, only the inclination of the transmitting antenna need be corrected for; i.e., for magnetic reception and 10° wire inclination, the VED fields need be reduced by only sin 10°/cos 10° ≈ 0.17 relative to the HED fields. Thus, at most distances, the HED and VED magnetic fields of an airborne transmitter differ by a factor of less than 3 for a transmitting antenna inclined at 45°, and are of comparable magnitude for an inclination of 10°. See Fig. 7.

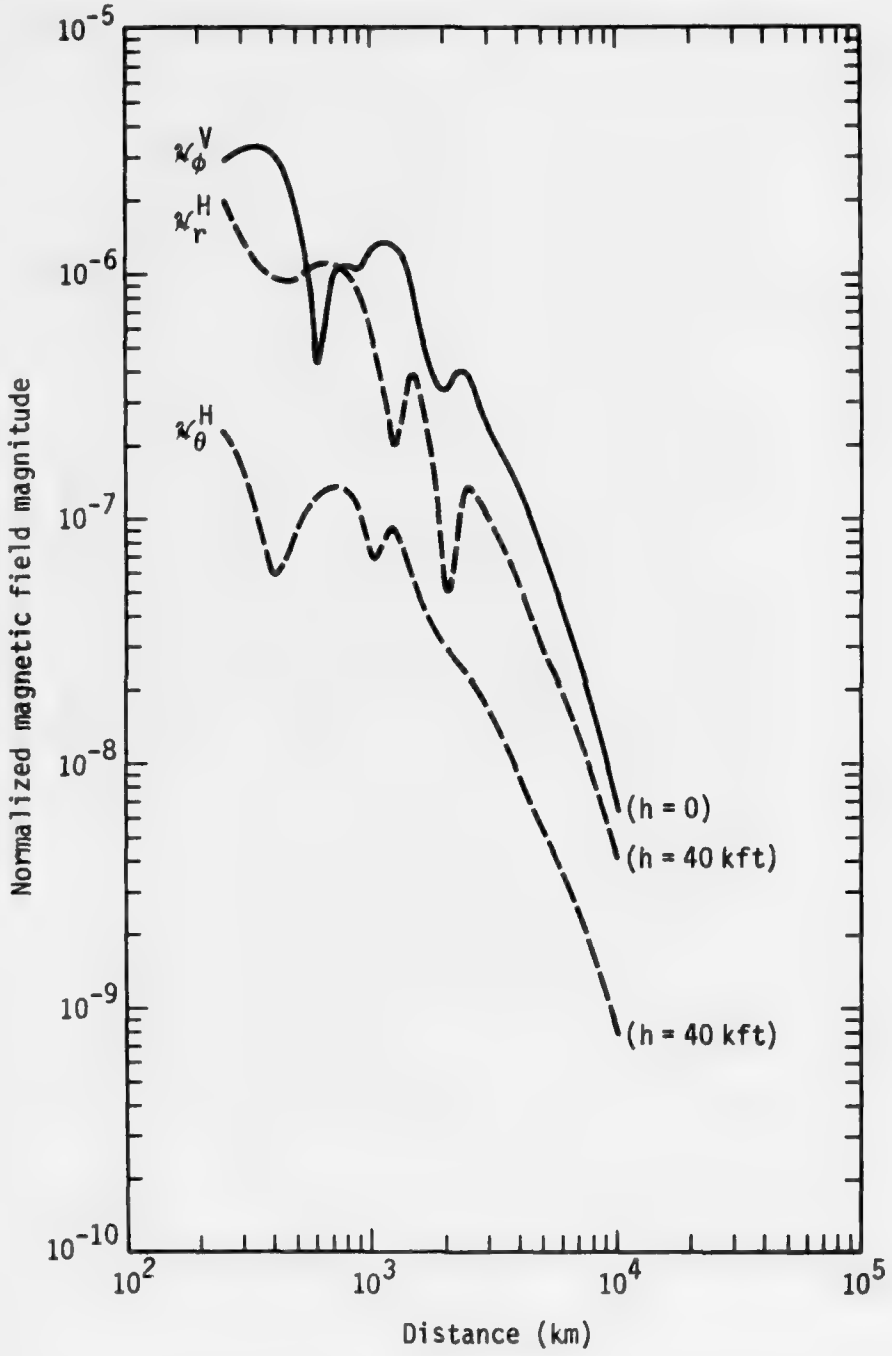

Figure 7. Magnetic field strength vs. distance for elevated VED and HED transmitters: 20 kHz, ambient day, $\sigma_g = 10^{-3}$ mhos/m.

Figure 8 is analogous to Fig. 6 (p. 22), but applies for a frequency of 40 kHz rather than 20 kHz. As indicated above, the HED results are not as accurate as for 20 kHz, because the higher modes are not much more heavily attenuated than the lower-order ones, and modes beyond $\alpha = 3$, $\beta = 2$ should probably be included. Nonetheless, the results in Fig. 8 should be sufficiently accurate for general conclusions. For antenna elevations of 40 kft and most distances, E_{ϕ}^{H} and E_{r}^{V} are comparable. Thus, after adjustments are made for a 10° trailing-wire antenna, the HED signal exceeds the VED signal by about 15 to 30 dB, depending on whether magnetic or electric receivers are used. Note from Figs. 1 and 5 (pp. 10 and 19) that, at 40 kHz, the second TE mode is excited about 20 dB more strongly than the first, but is attenuated only about 2 dB/Mm more quickly. Thus, out to about 10 Mm, E_{ϕ}^{H} as shown in Fig. 8 is composed mainly of the second TE mode.

When the fields are dominated by a single waveguide mode, the shapes of the field height-profiles are independent of distance from the transmitter, and are essentially the height-gain factors--suitably attenuated--of the dominant mode. For multimode propagation, the situation is much more complicated because the field height-profiles depend on the height-gain factors of two or more modes. The shape of these profiles depends on transmission range, because the relative contribution of each mode varies with distance.

To illustrate this effect, Fig. 9 shows height-profiles of the transverse HED electric field, E_{ϕ}^{H}, at four distances from a transmitter 15 kft above the ground. The curves apply to ambient day, 20 kHz, and $\sigma_g = 10^{-3}$ mhos/m. Recall that a total of five modes--$\alpha = 1,2,3$ and

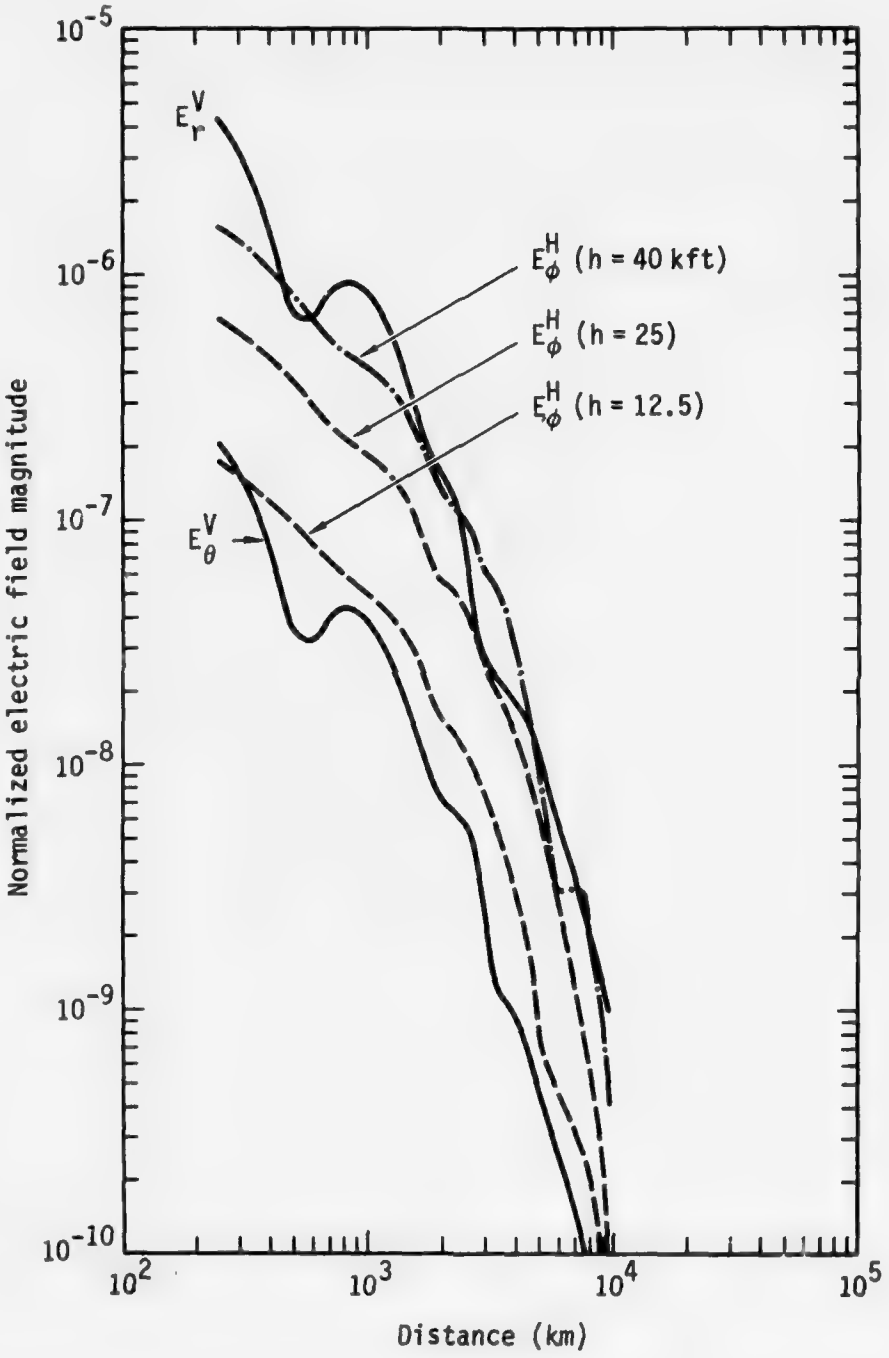

Figure 8. Electric field strength vs. distance for ground-based and elevated VED and HED transmitters: 40 kHz, ambient day, σ_g = 10-3 mhos/m.

β = 1,2--are used to calculate E_ϕ^H. Yet a comparison of Fig. 9 with Fig. 2 (p. 14) shows clearly that the mode structure evolves from the second TE mode at short distances to the first TE mode at large distances. Specifically, the profile at D = 700 km is similar to the β = 2 height-gain factor; the profile at D > 5000 km is similar to the β = 1 height-gain factor; and the profile at D ≈ 1500 km is a mixture between β = 1 and β = 2. A similar evolution with distance from higher to lower modes also occurs for the VED. The fact that the first TE mode becomes dominant at 20 kHz beyond a few Mm indicates that a sufficient number of modes has been retained in the mode sum. Apparently, this is not the case at 40 kHz, ambient day, $\sigma_g = 10^{-3}$ mhos/m, where the second TE mode dominates the first out to D ≈ 10,000 km.

Figure 10 shows the HED and VED electric field strengths for ground-based and elevated antennas, 20 kHz, ambient day, and $\sigma_g = 10^{-5}$ mhos/m, which is nominally representative of propagation over ice. The main differences between these results and those given in Fig. 6 (p. 22) for $\sigma_g = 10^{-3}$ mhos/m are: a) Fig. 10 shows generally lower field strengths at large distances than does Fig. 6, b) Fig. 10 shows larger values of E_θ^V and E_ϕ^H at h = 0, which occur because of the poorer ground reflection at $\sigma_g = 10^{-5}$ mhos/m, and c) E_ϕ^H generally compares more favorably with E_r^V at large distances in Fig. 10. Note, however, that the long-range results of Fig. 10 are artificial, because no regions of 10^{-5} mhos/m ground conductivity thousands of miles in extent exist on earth. The proper calculation would be a mixed seawater-ice path, which is beyond the scope of this report. The results of Fig. 10 are meaningful to distances of about 2000 km, which

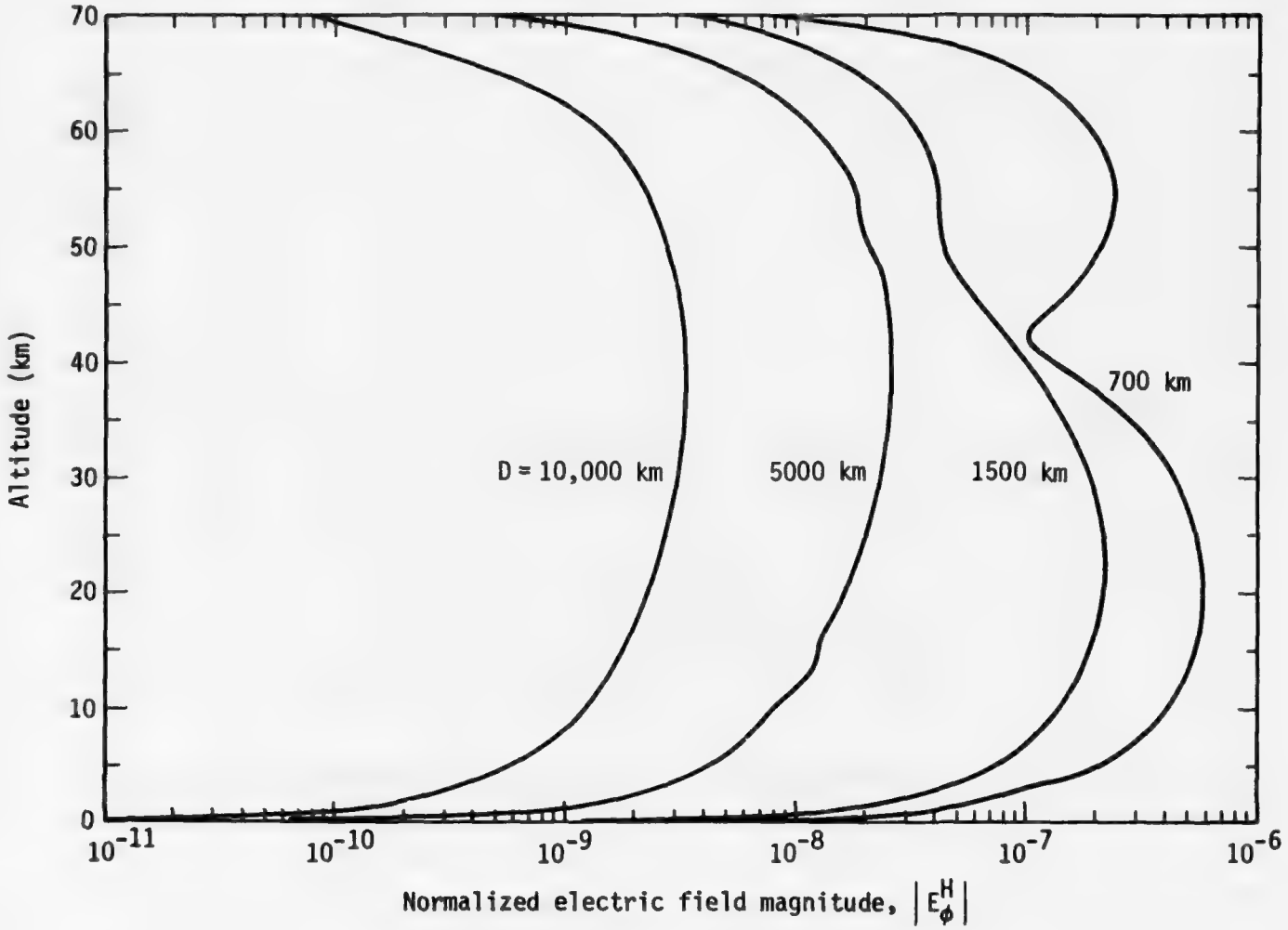

Figure 9. Profiles of electric field strength at several distances from an HED transmitter 15 kft above the ground: 20 kHz, ambient day, $\sigma_g = 10^{-3}$ mhos/m.

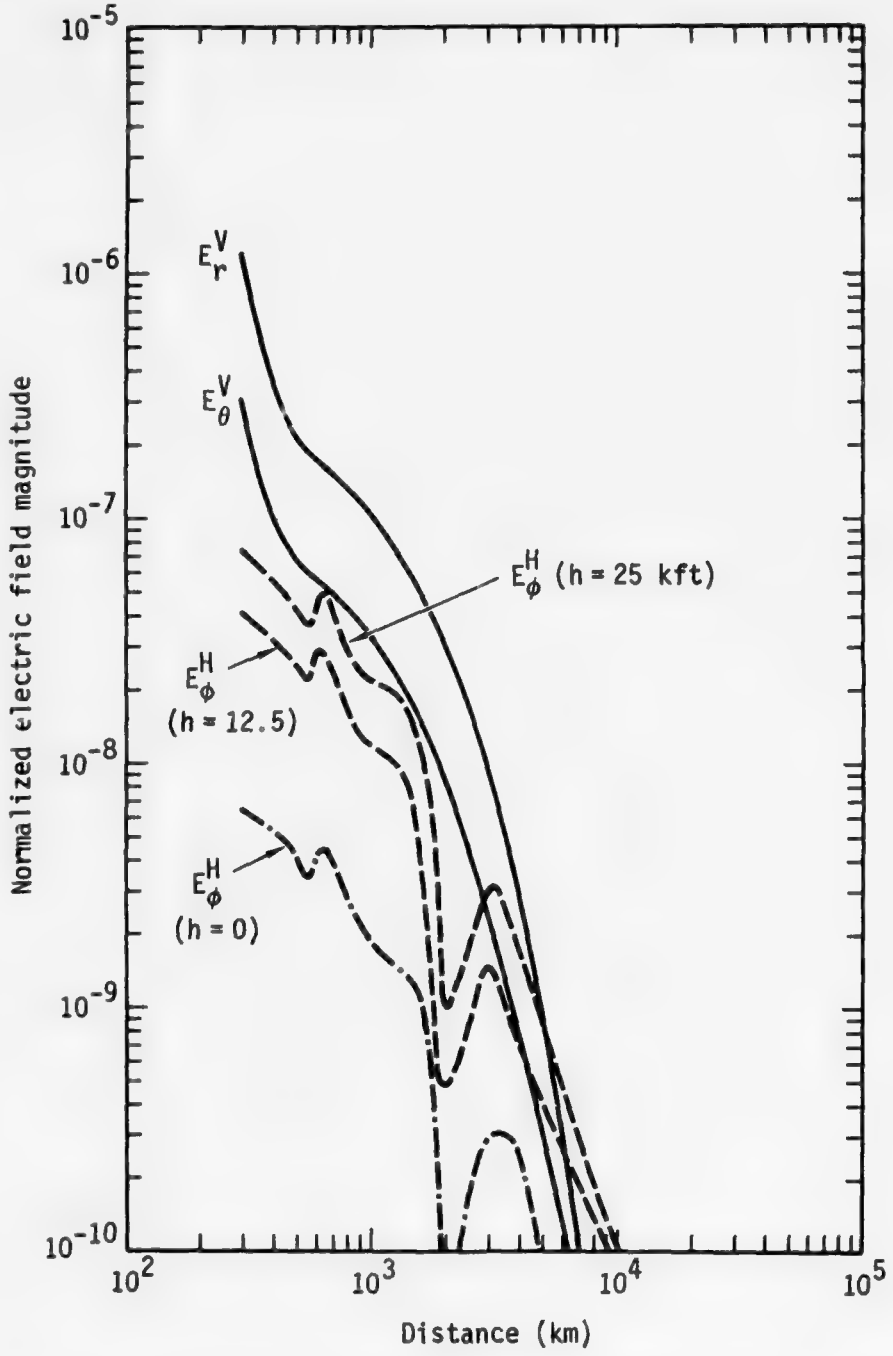

Figure 10. Electric field strength vs. distance for ground-based and elevated VED and HED transmitters: 20 kHz, ambient day, σ_g = 10^{-5} mhos/m.

is the length of Greenland. The excitation, height-gain, and attenuation factors given above for $\sigma_g = 10^{-5}$ mhos/m are, of course, applicable at any point having this ground conductivity.

Figures 11 and 12 show HED and VED electric field strengths versus distance for 20 and 40 kHz, $\sigma_g = 10^{-3}$ mhos/m, and a moderate spread-debris nuclear environment. Unlike ambient conditions, only a single TE and TM mode need be retained in the mode sum, since the higher modes are very highly attenuated. Thus, mode interference patterns are absent. The HED fields do not compare favorably with the VED fields for this disturbed environment, and, even for nearly horizontal electric-dipole transmitters and receivers, the HED signal would be smaller than the VED signal beyond a few thousand km. This behavior occurs because of the high attenuation of TE modes in disturbed environments.

For convenience in comparing performance for elevated antennas in ambient and disturbed environments, E_r^V and E_ϕ^H have been replotted on Fig. 13 for our ambient and spread-debris models, 20 kHz, $\sigma_g = 10^{-3}$ mhos/m, and h = 25 kft. The environmental degradation at the larger distances is apparent.

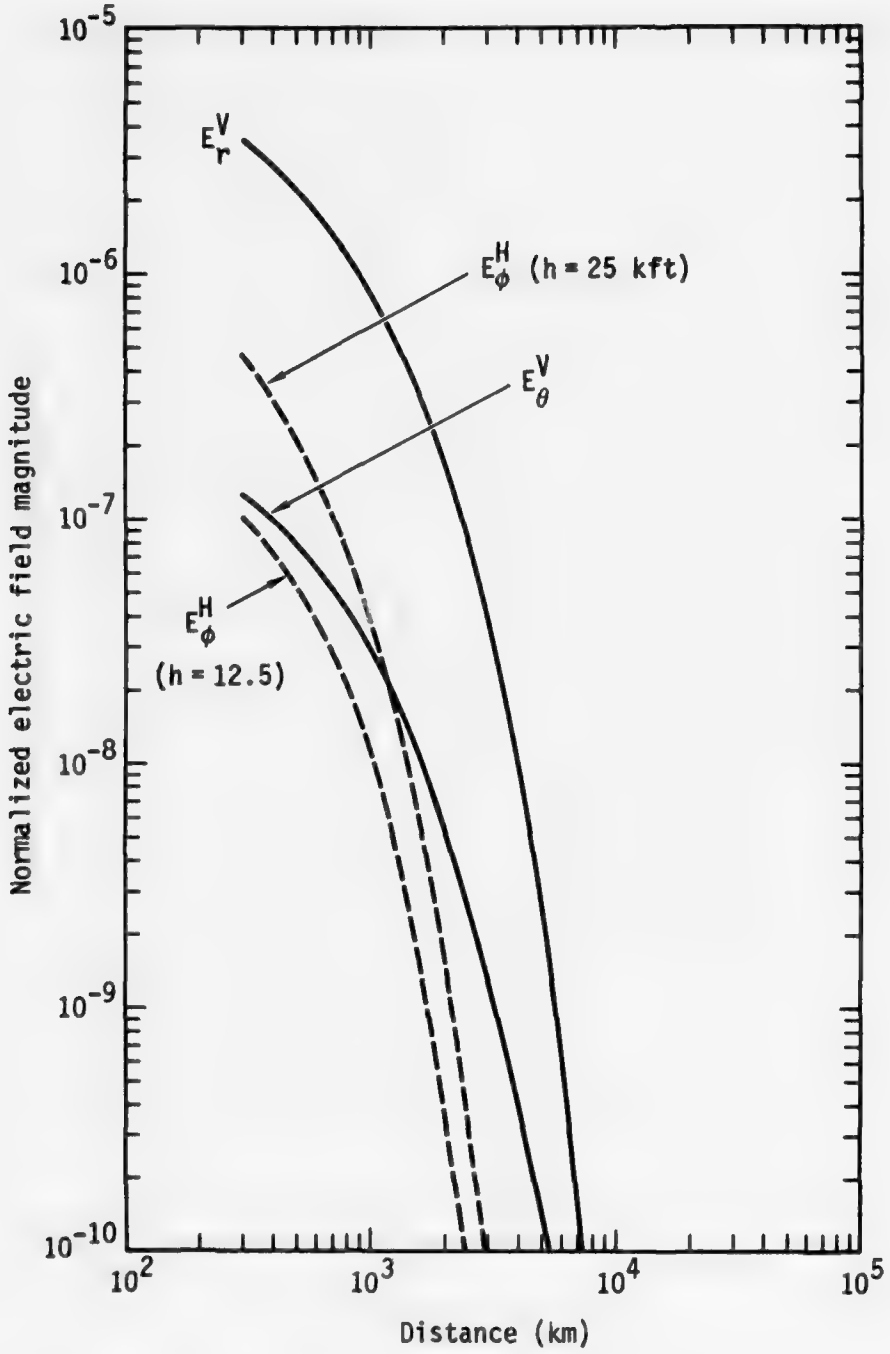

Figure 11. Electric field strength vs. distance for ground-based and elevated VED and HED transmitters: 20 kHz, moderate spread-debris environment, $\sigma_g = 10^{-3}$ mhos/m.

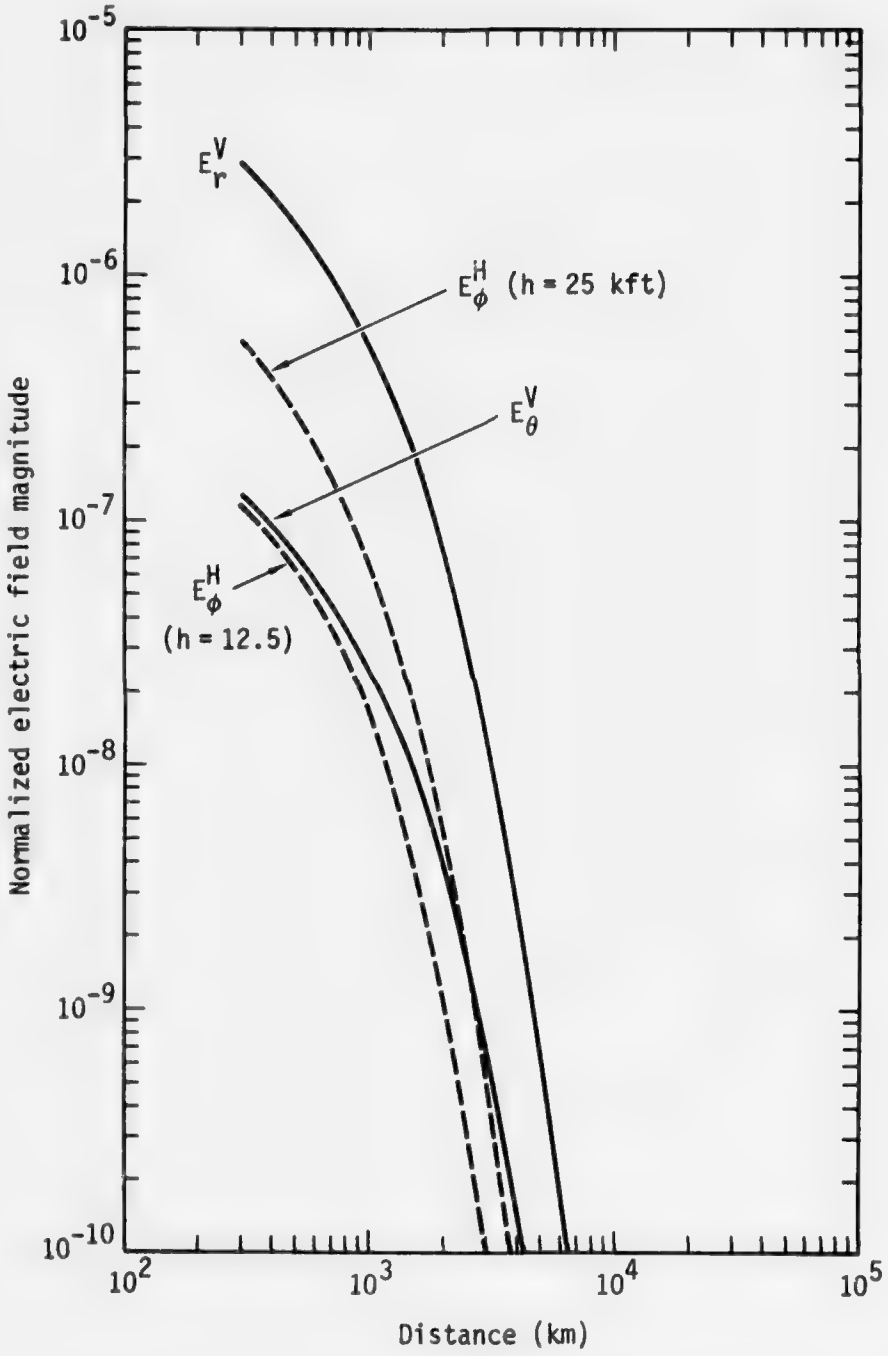

Figure 12. Electric field strength vs. distance for ground-based and elevated VED and HED transmitters: 40 kHz, moderate spread-debris environment, $\sigma_g = 10^{-3}$ mhos/m.

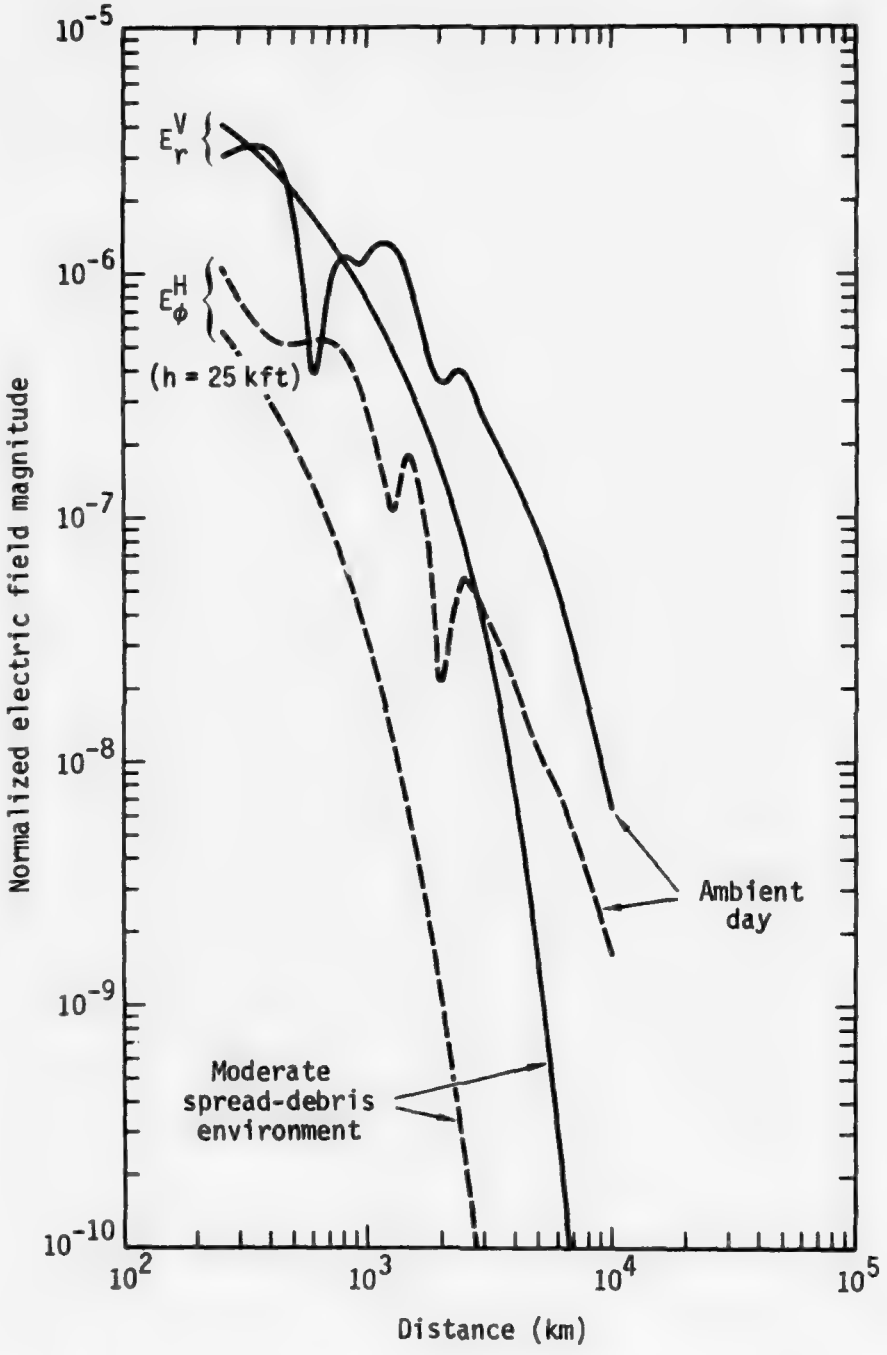

Figure 13. Electric field strength vs. distance for elevated VED and HED transmitters: 20 kHz, ambient and disturbed ionospheres, $\sigma_g = 10^{-3}$ mhos/m.

III. CONCLUSIONS

For antennas near the ground, the field components associated with TM modes are dominant, even for electric-dipole antennas inclined as little as 10° with respect to the horizontal. For a moderate spread-debris nuclear environment, the vertically polarized components again dominate the horizontally polarized components for all reasonable airborne-antenna inclinations, antenna elevations, and ranges beyond about 1500 km. This dominance occurs because of the high attenuation suffered by TE modes when ionospheric reflection-heights are severely depressed. For ambient conditions--and presumably for weakly disturbed conditions--the horizontally polarized components associated with TE-mode propagation are dominant for antenna elevations greater than 25 kft, and antenna inclinations smaller than about 20°, measured from the horizontal. For the frequencies considered, only slight "whispering gallery" modal characteristics are found.

APPENDIX

MATHEMATICAL SUMMARY

This appendix summarizes the equations used to obtain the numerical results given in the main text. These equations look very similar to those given by Galejs (*1972*). However, this resemblance is in appearance only, since we have fully accounted for earth curvature and vertical inhomogeneities in the ionospheric refractive index; Galejs assumed a sharply bounded ionosphere. Detailed derivations are not given in this appendix, but the mathematical development follows the work of Friedman (*1951*) fairly closely,* and the method of Budden (*1961*) is used to numerically solve the modal equations.**

REFRACTIVE INDEX

For computational purposes, the ionosphere is completely characterized by specifying the complex refractive index throughout the height-regions that govern long-wave propagation in the earth-ionosphere waveguide. This specification requires the number-densities, collision frequencies, and masses of each charged species present. Specifically, the refractive index, n, is given by

$$n^2(r) = 1 - \frac{e^2}{1837\varepsilon_o m_e} \sum_{\gamma} \frac{N_\gamma}{\omega(\omega - i\nu_\gamma) q_\gamma} \quad , \qquad \text{(A1)}$$

---

*Bernard Friedman, "Propagation in a Non-homogeneous Atmosphere," *Communications on Pure and Applied Mathematics*, Vol. 4, August 1951, pp. 317-350.

**K. G. Budden, *Radio Waves in the Ionosphere*, Cambridge University Press, 1961.

where ω is the wave-angular frequency, ϵ_o is the electric permittivity of free space, e is the electron charge, and m_e is the electron mass. The number density, N_γ, collision frequency, ν_γ, and atomic mass number, q_γ, of the γ^{th} species can be functions of altitude. The effects of the geomagnetic field have not been included in Eq. (A1), since, for the daytime or disturbed environments considered in this report, its effects on mode structure are negligible.

The analysis described below is quite general, and may be used for arbitrary height-dependences of N_γ and ν_γ. For VLF propagation in ambient daytime, however, only the electron terms need be retained in Eq. (A1). Moreover, the electron density, N_e, and collision frequency, ν_e, may be accurately represented by the following analytic forms over the height range of interest:

$$N_e = N_o \exp[b(z-H)] \tag{A2}$$

and

$$\nu_e = \nu_o \exp[-a(z-H)] \quad , \tag{A3}$$

where z and H are in kilometers. Since $\omega \ll \nu_e$ at the frequencies and altitudes of interest, it follows from Eq. (A1) that the imaginary part of the squared refractive index is proportional to N_e/ν_e and, hence, has an inverse scale height, $\beta = a + b$. Good approximations to actual daytime conditions are obtained by using $N_o = 3.93 \times 10^8$ el/m^3, $\nu_o = 5 \times 10^6$ sec^{-1}, $\beta = 0.5$ km^{-1}, and H = 70 km. In the notation of Wait (*1970*), these parameters correspond to a so-called "β=0.5, H=70" ionosphere. For the disturbed ionosphere, actual electron and ion

number-density and collision frequency profiles, taken from Field and Dore (*1975*), are used.

MODAL EQUATIONS

The fields of vertical and horizontal electric dipoles are composed of summations of elementary modes--so-called TM and TE modes--that propagate in the earth-ionosphere waveguide. The most difficult task in computing the fields is finding the eigenvalues of the dominant modes. Once these eigenvalues are known, it is straightforward--albeit somewhat tedious--to find excitation and height-gain factors, and to perform the mode summations to obtain the fields.

A spherical-polar coordinate system is used; the source is located at $\theta = 0$, and the waves travel in the θ-direction. Azimuthal (ϕ) symmetry may be assumed in determining the mode properties, because the effects of the geomagnetic field on mode structure are small for the environments considered. Of course, the ϕ-dependence of the total fields must be considered when mode excitation is calculated for the horizontal electric dipole (HED). Throughout the remainder of this appendix, the subscripts α and β will denote quantities associated with TM and TE modes, respectively. Unless otherwise noted, MKS units are used.

TM Modes

For TM modes, the electric and magnetic fields can be written

$$\underline{E}_\alpha = \left[\hat{e}_r E_{r\alpha}(r,\theta) + \hat{e}_\theta E_{\theta\alpha}(r,\theta)\right] e^{i\omega t} \qquad \text{(A4)}$$

and

$$\underline{H}_\alpha = \hat{e}_\phi H_{\phi\alpha}(r,\theta)\, e^{i\omega t} \quad . \qquad \text{(A5)}$$

For computational purposes, it is convenient to define the normalized wave admittance,

$$A_\alpha = \left(\frac{\mu_o}{\epsilon_o}\right)^{1/2} \frac{H_{\phi\alpha}}{E_{\theta\alpha}} \quad , \tag{A6}$$

and the related quantity

$$W_\alpha \equiv \frac{(A_\alpha - 1)}{(A_\alpha + 1)} \quad , \tag{A7}$$

where μ_o is the magnetic permittivity of free space. By substituting Eqs. (A4) and (A5) into Maxwell's equations and applying the constitutive relations, it follows, after some manipulation, that W_α is governed by the following equation:

$$\frac{dW_\alpha}{dr} = \frac{k}{2i}\left\{n^2(1-W_\alpha)^2 - \left[1 - \frac{a^2(1-C_\alpha^2)}{r^2n^2} + \frac{1}{4k^2r^2n^2}\right](1+W_\alpha)^2\right\} \quad , \tag{A8}$$

where $k = \omega/c$, c is the vacuum speed of light, a is the earth's radius, and n^2 is given by Eq. (A1). In Eq. (A8), the quantity C can be interpreted as the complex cosine of the incidence angle of the wave at the ground (i.e., at r=a). Solution of Eq. (A8) will satisfy the proper boundary conditions for only discrete values, C_α, of C. Hence, C_α is called the eigenvalue of the α^{th} TM mode. The boundary condition on W_α at the earth's surface determines C_α and is therefore called the modal equation. This modal equation is

$$W_\alpha(C_\alpha, r=a) = \frac{n_g^2 - \sqrt{n_g^2 - (1-C_\alpha^2)}}{n_g^2 + \sqrt{n_g^2 - (1-C_\alpha^2)}} \quad , \tag{A9}$$

where

$$n_g^2 = \varepsilon_g - \frac{i\sigma_g}{\omega\varepsilon_o} \quad , \tag{A10}$$

and ε_g and σ_g are the conductivity and relative dielectric constant of the ground, respectively. In Eq. (A9), the sign of the radical is chosen to correspond to a downgoing wave in the ground.

Data for N_γ, ν_γ, and q_γ are sufficient to determine n^2 as a function of height. Once n^2 is determined, Eqs. (A8) and (A9) form a closed set for W and C_α, and are solved by straightforward iteration. Each iteration requires the numerical integration of Eq. (A8), which is started at a great height where a purely upgoing wave is assumed as an initial condition. Thus, since the WKB (eikonal) solution may be used at great heights, the assumed value of W_α is given in terms of the refractive index, n_o, at the starting height, r_o, by

$$W(\alpha, r=r_o) = \frac{n_o^2 - \sqrt{n_o^2 - (1-C_\alpha^2)}}{n_o^2 + \sqrt{n_o^2 - (1-C_\alpha^2)}} \quad , \tag{A11}$$

where the sign of the radical is chosen to correspond to an upgoing wave. In practice, care is taken to choose a starting height so large that C_α is insensitive to its precise value.

Once C_α and, hence, $W_\alpha(r, C_\alpha)$ have been determined, it is a simple matter to calculate all electromagnetic parameters associated with a given mode. First, it is convenient to define

$$S_\alpha = \left(1-C_\alpha^2\right)^{1/2} \quad . \tag{A12}$$

Then, aside from a geometric spreading term, $H_{\phi\alpha}$ can be written

$$H_{\phi\alpha}(r=a) \propto \exp(-ikS_\alpha D) \quad , \tag{A13}$$

where D is the path length along the earth's surface. It follows from Eq. (A13) that attenuation rate, η, and phase velocity, V, are given by

$$\eta = 8.7 \times 10^6 k \; Im \; S \quad , \quad \text{dB/Mm} \tag{A14}$$

and

$$\frac{V}{c} = \frac{1}{Re \; S} \quad , \tag{A15}$$

where the subscript α has been suppressed. Equations (A13) through (A15) are valid beyond a few e-folding distances from the source and not too near the antipode.

TE Modes

The TE mode fields are

$$\underline{E}_\beta = \hat{e}_\phi E_{\phi\beta}(r,\theta) \; e^{i\omega t} \tag{A16}$$

and

$$\underline{H}_\beta = \left[\hat{e}_r H_{r\beta}(r,\theta) + \hat{e}_\theta H_{\theta\beta}(r,\theta)\right] \; e^{i\omega t} \quad . \tag{A17}$$

Define

$$A_\beta = \left(\frac{u_o}{\varepsilon_o}\right)^{1/2} \frac{H_{\theta\beta}}{E_{\phi\beta}} \tag{A18}$$

and

$$W_\beta = \frac{(A_\beta - C_\beta^2)}{(A_\beta + C_\beta^2)} \quad , \tag{A19}$$

whence

$$\frac{dW_\beta}{dr} = \frac{k}{2i}\left\{C^2(1+W_\beta)^2 - \frac{n^2}{C^2}\left[1 - \frac{a^2(1-C_\beta^2)}{r^2n^2} + \frac{1}{4k^2r^2n^2}\right](1-W_\beta)^2\right\} \quad . \tag{A20}$$

The starting value for the numerical integration of Eq. (A20) is

$$W_\beta(C_\beta, r=r_o) = \frac{\sqrt{n_o^2 - (1-C_\beta^2)} - C_\beta^2}{\sqrt{n_o^2 - (1-C_\beta^2)} + C_\beta^2} \quad , \tag{A21}$$

where the sign of the radical is chosen to correspond to an upgoing wave at r_o. The eigenvalue of the β^{th} TE mode is found from

$$W_\beta(C_\beta, r=a) = \frac{\sqrt{n_g^2 - (1-C_\beta^2)} - C_\beta^2}{\sqrt{n_g^2 - (1-C_\beta^2)} + C_\beta^2} \quad , \tag{A22}$$

where the sign of the radical is chosen to give a downgoing wave in the earth. The formulas for attenuation rate and phase velocity are identical with Eqs. (A12) through (A15), if C_β is substituted for C_α.

VERTICAL ELECTRIC DIPOLE

We consider a vertical electric dipole (VED) transmitter located at a distance, b, from the earth's center; h = b - a, then, is the altitude of the transmitter above the ground. The magnetic and electric fields of this transmitter are composed solely of elementary

TM waveguide modes, and are given by the following equations:

$$H_\phi^V = \frac{iI\ell a}{b}\sqrt{\frac{1}{D\lambda}}\sqrt{\frac{D/a}{\sin D/a}}\sum_\alpha \Lambda_\alpha S_\alpha^{1/2}\frac{e^{-ikS_\alpha D - i\pi/4}}{n^2(b)}G_\alpha(b)G_\alpha(r) \quad , \text{ AT/m} \tag{A23}$$

$$E_\theta^V = \frac{iIZ_o\ell a}{b}\sqrt{\frac{1}{D\lambda}}\sqrt{\frac{D/a}{\sin D/a}}\sum_\alpha \Lambda_\alpha S_\alpha^{1/2}\frac{e^{-ikS_\alpha D - i\pi/4}}{A_\alpha(r)n^2(b)}G_\alpha(b)G_\alpha(r) \quad , \text{ v/m} \tag{A24}$$

$$E_r^V = -\frac{iIZ_o\ell a^2}{n^2(r)br}\sqrt{\frac{1}{D\lambda}}\sqrt{\frac{D/a}{\sin D/a}}\sum_\alpha \Lambda_\alpha S_\alpha^{3/2}\frac{e^{-ikS_\alpha D - i\pi/4}}{n^2(b)}G_\alpha(b)G_\alpha(r) \quad , \text{ v/m} \tag{A25}$$

where I is the antenna current, ℓ is the effective antenna length, Z_o is the free-space impedance, and λ is the free-space wavelength. The TM-mode excitation factors are given by

$$\Lambda_\alpha = \left[2\int_a^\infty \frac{G_\alpha^2(r)dr}{n^2(r)}\right]^{-1} \quad , \ m^{-1} \tag{A26}$$

and the height-gain factors are given by

$$G_\alpha(r) = \frac{a}{r}\exp\left[-ik\int_a^r \frac{n^2(r')}{A_\alpha(r')}\,dr'\right] \quad . \tag{A27}$$

The admittance, A_α, is calculated from Eqs. (A7) and (A8).

Equations (A23) through (A27) comprise a generalization of those given by Galejs (*1972*, p. 97), which were derived assuming a uniform, sharply bounded ionosphere at a height H_o above the ground. The main advantage of the treatment given here is the allowance for an arbitrary ionospheric refractive-index height-profile in the solution of the modal equation, as discussed above. Moreover, the terms $A_\alpha(r)$, $n^2(r)$, and $n^2(b)$ in Eqs. (A23) through (A27) account for the fact that, at great transmitter or receiver heights, the fields are affected by the refractive index's not necessarily being unity in the vicinity of the antennas. Note that no "ionospheric height" appears in Eqs. (A23) through (A29), because, for arbitrary ionosphere height-profiles, an "ionospheric height" is an artifact that need not be defined in the treatment used here.

It is easy to show that Eqs. (A23) through (A27) reduce to the standard form for the often-used approximate model wherein the earth is assumed flat; the earth is a perfect reflector of infinite conductivity; and the ionosphere is a sharply bounded, perfect reflector of zero conductivity located at a height, h_o, above the ground. In this approximation, the refractive index at the transmitter or receiver must be unity, since the entire waveguide cavity is a pure vacuum. Thus, $n^2(r) = n^2(b) = 1$ in Eqs. (A23) through (A27). Also, the assumption of a flat earth implies $b/a = r/a = 1$. It is well known that the height-gain functions are of the form $\cos[(2\alpha-1)(\pi/2)z/h_o]$ in this approximation, whence Eq. (A26) gives

$$\Lambda_\alpha \to 1/H_o \quad , m^{-1} \quad . \tag{A28}$$

Equation (A27), which is a well-known result for VLF propagation in idealized sharply bounded waveguides, indicates that our excitation factor is, by necessity, normalized differently than that defined by Galejs (*1972*). Galejs factored the "ionospheric height" out of his excitation factor, which is thus dimensionless and of order unity. This factorization is not possible in our generalized treatment, since the artifact of an "ionospheric height" never enters. The result is that the excitation factors defined by Eq. (A26) are smaller than those of Galejs by a factor between 5×10^4 and 10^5.

HORIZONTAL ELECTRIC DIPOLE

The fields of a horizontal electric dipole are much more complex than those of the VED, since both TM and TE modes are excited. Moreover, the degree of excitation depends on the orientation of the dipole to the propagation path. Here, we will assume a dipole at $r = b$, $\theta = 0$, with its axis in the $\phi = 0$ direction. Thus, ϕ is the angle between the dipole orientation and transmission path direction.

The fields excited by an HED are given by the following equations:

$$E_\phi^H = -IZ_o \ell \sin\phi \left[\frac{-a^2}{kbr \sin\theta} \sum_\alpha \frac{F_\alpha}{A_\alpha(r) A_\alpha(b) S_\alpha^{3/2}} + \frac{ia}{b} \sum_\beta \frac{F_\beta}{S_\beta^{1/2}} \right] \quad , \text{ v/m} \tag{A29}$$

$$H_\theta^H = -I\ell \sin\phi \left[\frac{1}{kb \sin\theta} \sum_\alpha \frac{F_\alpha}{A_\alpha(b) S_\alpha^{3/2}} - \frac{ia^2}{br} \sum_\beta \frac{A_\beta(r) F_\beta}{S_\beta^{1/2}} \right] \quad , \text{ AT/m} \tag{A30}$$

$$H_r^H = \frac{-iI\ell a \sin\phi}{b} \sum_\beta S_\beta^{1/2} F_\beta \quad , \text{AT/m} \tag{A31}$$

$$E_r^H = \frac{iIZ_o \ell a \cos\phi}{b} \sum_\alpha \frac{S_\alpha^{1/2} F_\alpha}{A_\alpha(b)} \quad , \text{v/m} \tag{A32}$$

$$E_\theta^H = -IZ_o \ell \cos\phi \left[\frac{ia^2}{br} \sum_\alpha \frac{F_\alpha}{A_\alpha(r) A_\alpha(b) S_\alpha^{1/2}} - \frac{1}{kb \sin\theta} \sum_\beta \frac{F_\beta}{S_\beta^{3/2}} \right] \quad , \text{v/m} \tag{A33}$$

$$H_\phi^H = -I\ell \cos\phi \left[\frac{ia}{b} \sum_\alpha \frac{F_\alpha}{A_\alpha(b) S_\alpha^{1/2}} - \frac{a}{kbr \sin\theta} \sum_\beta \frac{A_\beta(r) F_\beta}{S_\beta^{3/2}} \right] \quad , \text{AT/m} \tag{A34}$$

where the propagators for the TM and TE modes are given by

$$F_\alpha = \sqrt{\frac{1}{D\lambda}} \sqrt{\frac{D/a}{\sin D/a}} \Lambda_\alpha \frac{e^{-ikS_\alpha D - i\pi/4}}{n^2(b)} G_\alpha(b) G_\alpha(r) \tag{A35}$$

$$F_\beta = \sqrt{\frac{1}{D\lambda}} \sqrt{\frac{D/a}{\sin D/a}} \Lambda_\beta e^{-ikS_\beta D - i\pi/4} G_\beta(b) G_\beta(r) \quad . \tag{A36}$$

All symbols have been defined earlier in this appendix, except for the TE-mode excitation factor and height-gain function, which are given by

$$\Lambda_\beta = \left[2 \int_a^\infty G_\beta^2(r) dr \right]^{-1} \tag{A37}$$

and

$$G_\beta(r) = \frac{a}{r} \exp\left[ik \int_a^r A_\beta(r')dr'\right] \quad . \tag{A38}$$

Equations (A29) through (A38) represent generalizations of the relations given by Galejs (*1972*, p. 99) in that they account for arbitrary height-gradients of the ionospheric height-gradients.

For arbitrary values of ϕ, all six field components are radiated by the HED. For broadside orientation ($\phi = \pi/2$), only H_r, E_ϕ, and H_θ are radiated; whereas, for end-fire orientation, E_r, E_θ, and H_ϕ are radiated. However, even though these orientations produce the same field components as exist in TE and TM modes, the fields are not pure modes. For example, even for $\sin \phi = 1$, Eqs. (A29) through (A31) show that only H_r is composed solely of TE modes. E_ϕ and H_θ contain contributions from both TE and TM modes. Thus, broadside fields from an HED are often called quasi-TE modes and end-fire fields are called quasi-TM modes.

REFERENCES

Budden, K. G., *Radio Waves in the Ionosphere*, Cambridge University Press, 1961.

Field, E. C., and M. Dore, *VLF/LF TE-Mode Propagation Under Disturbed Ionospheric Conditions*, Air Force Cambridge Research Laboratories, AFCRL-TR-75-0382, July 1975.

Friedman, B., "Propagation in a Non-Homogeneous Atmosphere," *Communications on Pure and Applied Mathematics*, Vol. 4, August 1951, pp. 317-350.

Galejs, J., *Terrestrial Propagation of Long Electromagnetic Waves*, Pergamon Press, New York, 1972.

Pappert, R. A., "Effects of Elevation and Ground Conductivity on Horizontal Dipole Excitation of the Earth-Ionosphere Waveguide," *RADIO Science*, Vol. 5, No. 3, March 1970, pp. 579-590.

Wait, J. R., *Electromagnetic Waves in Stratified Media*, Pergamon Press, New York, 1970.

Wait, J. R., and K. P. Spies, *Characteristics of the Earth-Ionosphere Waveguide for VLF Radio Waves*, U.S. Department of Commerce, National Bureau of Standards, Tech. Note 300, 1964.

MISSION
of
Rome Air Development Center

RADC plans and conducts research, exploratory and advanced development programs in command, control, and communications (C^3) activities, and in the C^3 areas of information sciences and intelligence. The principal technical mission areas are communications, electromagnetic guidance and control, surveillance of ground and aerospace objects, intelligence data collection and handling, information system technology, ionospheric propagation, solid state sciences, microwave physics and electronic reliability, maintainability and compatibility.

Printed by
United States Air Force
Hanscom AFB, Mass. 01731